# Rotational Energy Harvesting To Prolong Flight Duration Of Quadcopters

**By**

**Moses Amoasi Acquah**

**(10249555)**

**This Thesis/Dissertation Is Submitted To The University Of Ghana, Legon In Partial Fulfillment Of The Requirements For The Award Of MPhil Computer Engineering Degree.**

**July 2014**

## DECLARATION

I, Moses Amoasi Acquah, hereby declare that this thesis document except where indicated by referencing, is my own work carried out under supervision in the Department of Computer Engineering, Faculty of Engineering Sciences, University of Ghana, Legon. I further declare that this thesis, either in whole or in part, has not been presented for another degree in this University or elsewhere.

7th April 2015

…… ……

Moses Amoasi Acquah Date

(Student)

…… ……..

Dr Robert A. Sowah Date

(Major Supervisor)

6th April 2015

…… ……

Dr Nathan Amanquah Date

(Co-Supervisor)

## ACKNOWLEDGEMENT

I would like to express my deepest gratitude to my supervisors, Dr. Robert A. Sowah and Dr. Nathan Amanquah for their patient guidance, enthusiastic encouragement and useful critiques of this research work. Thank you very much for the time you contributed to this work.

I wish to thank various individuals who assisted me in the form of academic collaborations and technical expertise; Special Thanks Dr. A. Mills for his invaluable discussions, advice and guidance on the model equation and also for allowing me to use his lab. I also need to express my sincere gratitude to Dr. Isaac K. Nti for his continuous support, opinions and recommendations, I am also grateful for his assistance in keeping my progress on schedule.

My special thanks are extended Fiona Naa Sackey for her support and contribution. I wish to thank all my classmates and friends for their support, encouragement and the humour that cheered me on.
Finally, I wish to thank my Family for their sacrifice and support throughout my study, without your encouragement I would not have come this far.

Moses Amoasi Acquah.

**Rotational Energy Harvesting To Prolong Flight Duration Of Quadcopters**

## ABSTRACT

This thesis presents a rotational energy harvester using brushless direct current (BLDC) generator to harvest ambient energy for quadcopter in order to prolong it flight duration. Quadcopters also known as drones are developed with the intention of operating in conditions where the presence of an on-board human pilot is either too risky or unnecessary, as such they are broadly referred to as UAV (Unmanned Aerial Vehicles). For a drone its endurance is essential in order to achieve operational goals, because most electrically powered drones have a limitation on size and mass, due to this they cannot carry a large mass of on-board energy thereby having short flight time. Quadcopters have a lot benefits such as large amount of controllability, hovering and manoeuvrability, because of this they are suitable for both indoor and outdoor applications such as scientific research, security surveillance and reconnaissance.

BLDC generators are coupled with the propellers of the quadcopter to transfer kinetic energy from the propellers to the generator. Taking into consideration the power requirement of quadcopter, the output of the generator is amplified using DC-DC boost and regulated to power and charge the on-board battery.

The BLDC generator was simulated in MATLAB/SIMULINK, monitor and analyse the output of the generator.

A final prototype of the rotational energy harvesting system was built and this comprised a quadcopter, power management system and a charging system.

Results from the test conducted on the system produced output power levels of 4.98W at a source rotation speed of 5400RPM, which is use to augment the primary power supply. In all about 30% more energy was harvested from 4 micro-generators connected in parallel. This translates to about 10 minutes increase in flight endurance, thus a gain of about 50% in flight duration.

# TABLE OF CONTENTS

## LIST OF FIGURES

## LIST OF TABLES

# LIST OF ABBREVIATIONS

| | |
|---|---|
| 3s | Three Cells |
| AC | Alternating Current |
| BLDC | Brushless Direct Current |
| CNT | Carbon Nano Tubes |
| DC | Direct Current |
| DC-DC | Direct Current to Direct Current |
| EMF | Electromotive Force |
| ESC | Electronic Speed Controllers |
| GPS | Global Positioning System |
| GSM | Global System for Mobile |
| IC | Integrated Circuit |
| IMU | Inertial Measurement Unit |
| LED | Light Emitting Diodes |
| LiPo | Lithium Polymer |
| MAV | Micro Air Vehicle |
| MFC | Macro-Fiber Composite |
| MMF | Magneto-Motive-Force |
| NCG | Nanocomposite Generator |
| NP | Nanoparticles |
| PCB | Printed Circuit Board |
| PFC | Piezo-Fiber Composite |
| PFM | Pulse Frequency Modulation |
| PM | Permanent Magnet |
| PPM | Pulse Position Modulation |
| PWM | Pulse-Width Modulation |
| PZT | Lead Zirconate Titanate |
| RC | Remote Control |
| RFID | Radio Frequency Identification |
| RGO | Reduced Graphene Oxide |
| RPM | Revolutions Per Minute |
| SMD | Surface Mount Devices |
| UAV | Unmanned Aerial Vehicles |

# CHAPTER 1

# INTRODUCTION

## 1.1 Introduction

Energy harvesting from moving structures has been a topic of much research, particularly for applications in electrically powered UAVs like the quadcopter.

In recent applications it is very advantageous to scavenge energy from ambient sources, since most of these energy sources have energy in abundance.

Most researchers have looked into improving the endurance of electrically powered UAV's (Unmanned Aerial Vehicles) also known as drones using energy harvesting technologies such as photovoltaic harvesting and vibration harvesting. However, none of their works reported on a design to harvest energy directly from continuous rotation of the UAV. This is an important application for indoor use of drones, since energy harvesting using solar has been developed extensively and efficiently for outdoor application of drones where ambient luminance is in abundance but cannot operate efficiently indoors.

The motivation behind this thesis is to investigate rotational energy harvesting from the rotor of quadcopters using BLDC (Brushless DC) generator as a transducer to prolong the flight duration.

Compared with other generators, the BLDC generator has lots of benefits; it is lightweight, it has a compact design, and low maintenance because it has a magnetic source inside itself [1].

Simulation of the system has been developed to validate the proposed method, and experimental results prove the proposed methods.

This chapter presents the background of UAV's and energy harvesting process; it also throws light on overview of the problem definition, objectives and relevance of this research. The outline of the thesis is also discussed.

## 1.2 Background

The development of small electrically powered drones has gained tremendous interest in the research community. One particular area of interest involves creating innovative techniques to increase the flight duration or endurance of UAVs. Since energy harvesting technology presents a potential solution for the improvement of flight duration by converting ambient energy into electrical energy that can be used to power the UAV.

The concept of using harvested energy to power UAV is not new, energy harvesting techniques can be classified as kinetic and non-kinetic with examples being photovoltaic harvesting and vibration harvesting respectively. Generally vibration harvesting such as rotational harvesters are based on electromagnetic transduction techniques and are used in numerous applications from bicycle dynamos to large-scale power generation as in hydroelectric power plants. Well-designed generators, such as the BLDC generator can be very efficient at converting rotational energy into electrical energy.

The UAV or Drone is an aircraft without a human pilot on-board. Its flight is either controlled autonomously or by a ground base that is either a computer or joystick controller.

UAV have lots of advantages and can be categorized as fixed-wing aircraft with example being the plane or glider UAV and rotary-wing aircraft with example being multi-rotor UAV.

Comparing the two, rotary-wing aircrafts have specific characteristics like vertical take-off and landing in limited space, easy to control, hovering and manoeuvrability makes them suitable for both indoor and outdoor applications and this may be impossible to be performed using fixed-wing aircrafts. Consequently, the choice of

rotary-wing (quadcopter) over fixed-wing UAV in this work is based on these advantages.

### 1.2.1 Energy Harvesting Transduction Process

To extract power from ambient energy sources a transducer is required in order to obtain usable electrical power. Two sources from which energy from ambient sources can be harvested are kinetic and non-kinetic sources, with these and via transducer, energy can be converted into usable electrical power. Kinetic energy sources rely on ambient motion or more specifically vibrations that are present in an environment or host structure as presented in [3] and [4]. On the other hand, non-kinetic energy sources include electromagnetic waves from solar energy, thus radiation of the sun. Table 1.1 provides an indication of typical power levels along with the conditions assumed.

From the table it is obvious that density of solar power in outdoor conditions is very high compared to that of vibration harvester. However, it becomes comparable with the other sources if used indoors and is not suitable for embedded applications or dirty environments where the cells can become obscured [5]. The output of energy harvester takes the form of varying electrical voltage and current. Currently most energy harvesters have had a paradigm shift from a single ambient source harvesting

to the hybrid, where energy is harvested from two or more source such as from solar and vibration as discussed in [6].

**Table 1.1 Typical data for various energy harvesting sources reproduced from [2]**

| | Conditions | Power densities | Area of Volume | Energy/Day |
|---|---|---|---|---|
| Vibration | $1m/s^2$ | $100\mu W/cm^3$ | $1cm^3$ | 8.64J(Continues) |
| Solar | Outdoors | $7{,}500\mu W/cm^3$ | $1cm^2$ | 324J(50% light) |
| Solar | Indoors | $7{,}500\mu W/cm^3$ | $1cm^2$ | 4.32J(50% light) |

To convert energy form one source to another a transducer used, its purpose is to extracting energy from an ambient source and converting it into usable electrical power. Kinetic energy harvesters employ various transducers such as piezoelectric, electromagnetic to harvest ambient energy from the surrounding.

A piezoelectric transducer is a cantilever beam, made up of a layer of deposited piezoelectric material such as Lead Zirconate Titanate also known as PZT (unimorph and bimorph when there exist one layer and two layers respectively). One end of the

beam is made stationary and the other free, a mass is then attached to the free end of the beam [3]. The harvester operates by applying mechanical force on a PZT device, this induces electrical charge on the piezoelectric capacitance and voltage is induces across the terminals of the device [4]. On the other hand a piezoelectric actuator will experience a mechanical force when a voltage is applied across the device terminals. Figure 1.1shows a schematic of the piezoelectric cantilever beam.

The conversion of mechanical energy into electrical power depends on the piezoelectric coupling coefficient, $k_{ij}$, and the capacitance of the piezoelectric material, $C_p$. The subscripts $i$ and $j$ in the coupling coefficient represent the polarisation of the material in three-dimensional space [5].

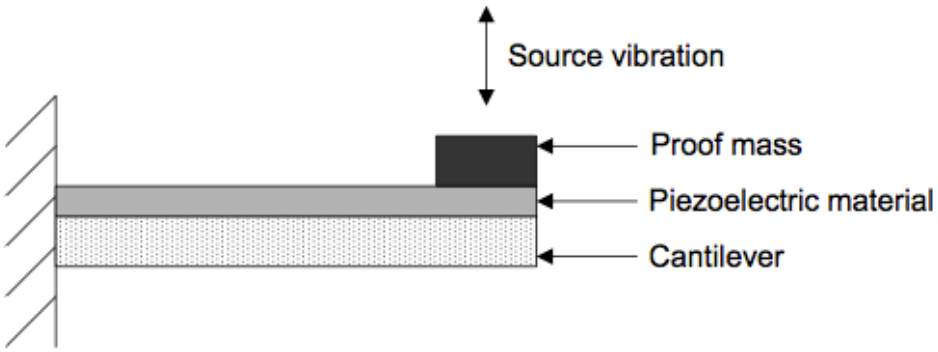


**Figure 1.1: A unimorph piezoelectric cantilever beam**

The piezoelectric transduction mechanism is employed in order to harvest vibration energy from the surrounding.

Kim et al in [6] published a 1 mm thick cymbal transducer made up of ten PZT layers stacked under a steel cymbal shaped enclosure is used to harvest vibrational energy as

in Figure 1.2. When subjected to rigorous vibration an out of 250V is recorder from its terminals. A DC-DC buck converter is used to step down the 250V, by matching the impedance of the buck converter to that of the transducer a maximum of 25V was obtained. The output voltage was used to power eighty-four LED (Light Emitting Diode) arranged in a combination of series and parallel. A total power consumption of 53mW was recorded from the LEDs. This work did not implement a means of storage as an auxiliary power supply should the harvester goes out.

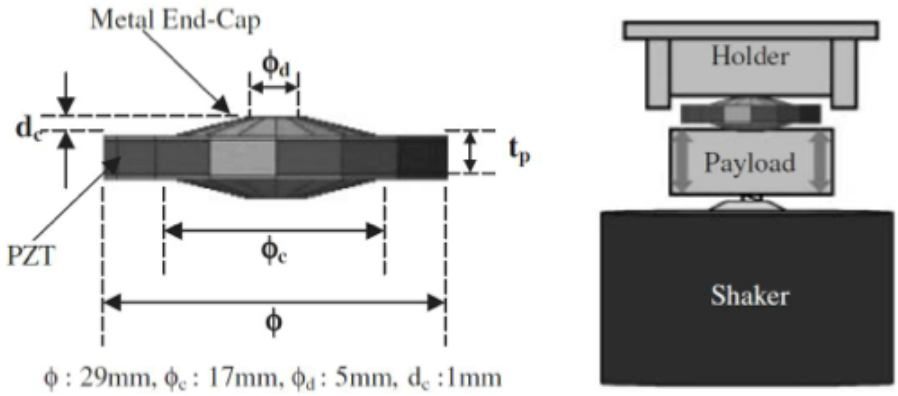


**Figure 1.2: A cymbal-shaped piezoelectric transducer reproduced from [7][6].**

Two cantilevered-designs of a piezoelectric vibration-powered generator prototype each with a dimensions of 15mm × 6.7mm and 30mm × 3.6mm, produced an output power of 375µW into a resistive load from an excitation source accelerating at $2.5ms^{-2}$ with a frequency of 120Hz [7]. The authors modelled the mechanical parts of the piezoelectric generator with equivalent electrical components; thus, the mass was represented as an inductor, mechanical stiffness as a capacitor and the mechanical

damping as a resistor. The output voltage from the transducer was rectified using a diode rectifier and used to charge a $4.7\mu F$ storage capacitor and a radio set.

The work by Shenck and Paradiso in [8] reported on two methods used in harvesting energy from a shoe using piezoelectric energy harvester. The first methods uses a hexagonal-shaped piezoelectric material to harvest energy during the bending of the ball of the foot as a person walks while the second approach uses a bimorph piezoelectric plate positioned under the heel to scavenge energy when the heel of the shoe strikes the ground. In both methods mechanical excitations in the form of strain is transferred to the piezoelectric device as the wearer walks. This produces about $1.3mW$ and $8.4mW$ of average power under matched conditions respectively. The output voltage of the power management circuit was used to power a RFID (radio frequency identification) tag. Part of the generated energy is used to charge a storage capacitor. The authors used forward switch mode converter in place of a low-dropout linear regulator in order to achieve a battery-less application, since switch mode converters are more efficient taking into consideration the large difference between the voltage from the piezoelectric transducer (about 170V) and the load voltage (5V). A prototype of the shoe-mounted piezoelectric energy harvesting system is shown in Figure 1.3.

**Figure 1.3: A shoe-mounted piezoelectric energy harvesting by [9].**

Park et al in [9] presented a new energy harvesting method using thin film- type nanogenerators with perovskite ceramic materials (PbZrxTi1-xO3 and BaTiO3) piezoelectric materials that can convert vibrational and mechanical energy sources from human activities such as pressure, bending, and stretching motions into electrical energy. BaTiO3 thin film nanogenerator has been demonstrated by this work using the transfer process of high temperature annealed perovskite thin film from bulk substrates onto flexible substrates; it generates a much higher level of power density than other devices with a similar structure.

This paper reports on the nanocomposite generator (NCG) as achieving a simple, low-cost, and large area fabrication based on BaTiO3 nanoparticles (NPs) synthesized via a hydrothermal reaction and RGO (Reduced Graphene Oxide).

The BaTiO3 NPs generate piezoelectric potential under external stress and act as an energy generation source. The CNT's role in an NCG device as dispersant, stress reinforcing agent,

Under continual bending and unbending cycles, the NCG device repeatedly generates an open-circuit voltage (Voc) approximately 3.2V and a short-circuit cur-rent (Isc) signal of 250 to 350nA; these output values are produced for a maximum horizontal displacement of 5mm from an original 4cm long sample at a deformation rate of $0.2ms^{-1}$.

The authors demonstrated the lit up of a commercial LED solely with the electricity generated from the NCG device. The authors did not mention an implementation of a power management circuit to transfer regulated power to the load and also no energy storage device is implemented.

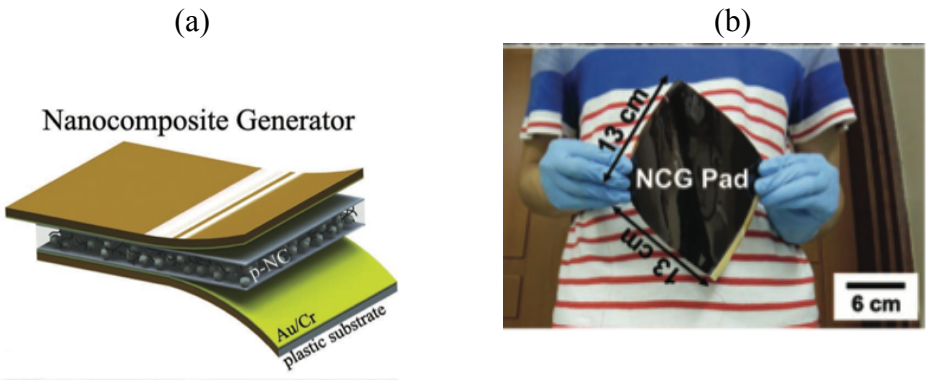


**Figure 1.4: Structure of Nanocomposite Generator, (b) Size of NCG pad.**

The work by Holmes et al [10] reports on a harvesting rotational energy from flow sensing applications using a small sized axial-flux PM (permanent magnet) electromagnetic generator of about $7.5mm$ in diameter. The generator is made up of two silicon stators with a permanent magnet rotor sandwiched between the stators.

The harvester device as in Figure 1.5 delivers an output power of 1.1mW per stator at a rotation speed of 30000RPM. The authors reported that the output power of the generator scales to $L^5$, where L is any characteristic linear dimension of the generator. As an example the work demonstrated that for a cm scale device the output is $1mW$, scaling the device down by a factor of four will result in an output of $10\mu W$, thus reduction in PM generator size would reduce output power density, unless the rotation speed of the rotor is very much increased.

(a) (b)

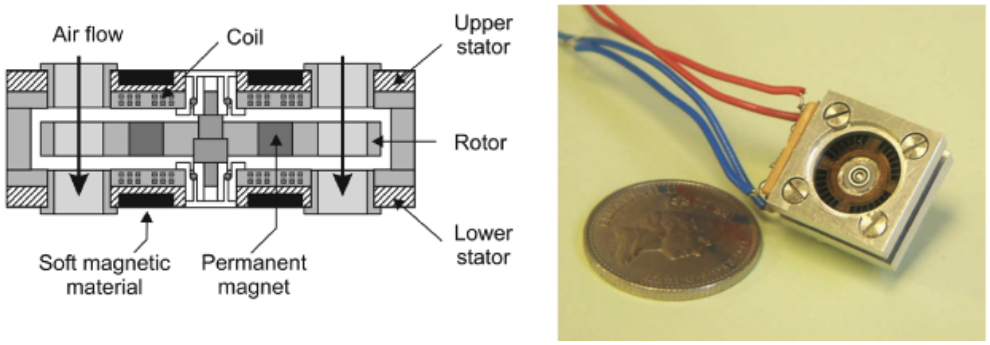


**Figure 1.5: An axial-flux permanent magnet generator [10], (a) Schematic cross section through device. (b) Prototype of the device.**

The work by [11] presented a formulation that describes the scaling of transducer parameters. Each parameter of the transducer can be represented by a scaling variable, L, which is a linear dimension of the device. To throw more light the author stated that the mass of an object, m, scales as $L^3$ since the mass' density is proportional to its volume whereas a frictional force, F, scales as $L^2$ since it is dependent on the area of the mass in contact with a surface, therefore from Newton's third law, $F = ma$, the acceleration, a, of a mass across a surface will scale as $L^{-1}$. Forces that scale as $L^2$ might result in an output power per unit volume that scales as $L^{-1}$. Reducing the dimension by a factor of ten will result in a ten times increase in the output power per unit volume.

From [10], at a constant speed ω, the output power P, for a generator on a resistive load is expressed as $P \propto \frac{{V_{out}}^2}{R}$, where $V_{out} \propto L^2\omega$ and $R \propto L^{-1}$. Therefore, output power scales as $L^3\omega^2$. For a constant rotation speed, the power density of the generator will scale as $\omega^2$, i.e. independent of the linear dimensions of the generator.In [12], Raisigel et al presented an 8mm diameter axial-flux permanent magnet microgenerator (Figure 1.6) with a stator made of three-phase planar coils. The harvester setup delivered a maximum output power of 5W with an efficiency of 66% at stator speed of 380 $kRPM$ hen a 12Ω resistive load is applied at its terminals. The authors reported that a high electrical efficiency of 95% was achieved in a test but

resulted in an output power of 1.2W at $399kRPM$. The output of the microgenerator was converted to DC (Direct Current) using an AC/DC synchronous rectifier and a step-up converter was used to boost the generator's output power. The generators output power peaked at 12Ω and decreased with an increase or decrease in this value. The authors stated that higher electrical efficiencies could be achieved if the resistance in the stator coils was reduced but this condition cannot guarantee that maximum power be transferred from the microgenerator to the load.

In [13], Trimmer and Gabriel stated that ω scales as $L^{-1}$. In order words, smaller rotary devices will be able to achieve higher rotational speeds than their larger

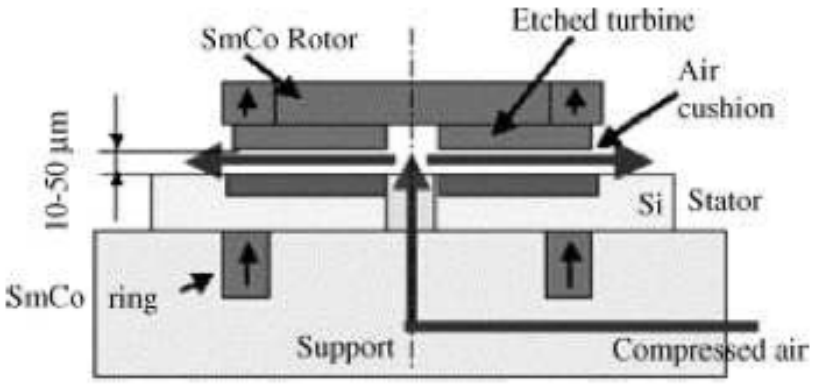


**Figure 1.6: Side view of the microgenerator from [12].**

counterparts. This implies that the output power from a rotational generator will scale as L. When this is compared to the output power from a vibration-driven inertial energy harvester, $\frac{Y_0 Z_l m\omega^3}{2}$, which scales as $L^2$, a rotational energy harvester will produce output power levels which are an order of magnitude larger than their vibration counterparts for a given device volume.

#### 1.2.1.1 Discussion

The above reviews reported on the transduction mechanism for vibration harvester and flow rotational harvesters, which are used as a guideline for the work on the rotational energy harvester.

In most of the review it was reported that in order to transfer power from a transducer to a load the impedance of the load should be greater than that of the transducer since the contrary will lead to overheating and destruction of the transducer. It was also evident that in order to transfer maximum power then the impedance of the transducer should be matched to that of the load. Energy storage elements are a fundamental requirement for an energy harvester; a hybrid system can be employed in a case where the power produced by the transducer is not enough to power the system electronics. Lastly in the case of micro-electromagnetic generator, reducing the size of the generator scale the output power, giving rise to lower power densities.

### 1.2.2 Power Management System

Power management systems have the fundamental requirement in energy harvesting system to charge a storage device and to conserve energy. Also they have the requirement to switch certain parts of a system off or switch them into a low-power state when they are not being utilized as in Figure 1.7.

From the reviews above power management electronics are required to interface energy harvesters to achieve the following:

• In power electronics for harvesters the input impedance of the interface electronics need to be controlled to match that of the transducer in order to transfer high power from the transducer to the load.

• There need to be a voltage regulation since the output voltage and current from the energy harvester might not be compatible with the load electronics.

• Energy storage is a major requirement in energy harvesting systems, it is to remedy any effects of intermittency from the ambient energy source so does not affect the continuous operation of the system.

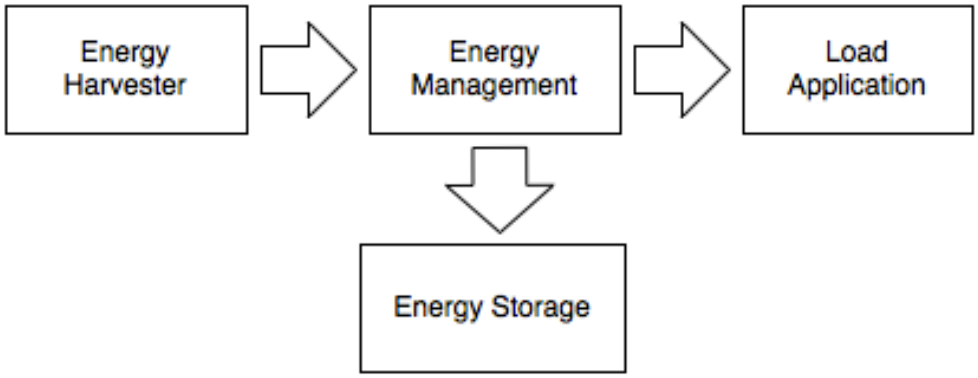


**Figure 1.7: Topology for energy harvesting systems.**

### 1.2.3 Efficient Energy Transfer Requirements

To ensure that the energy produced in the electrical generator is efficiently transferred to the load, the impedance of the load should be larger than the impedance of the generator, as in Figure 1.8(a). Although the configuration $Rload \gg Rsource$ achieves the maximum electrical efficiency and prevents the generator from thermal destruction, it does not achieve the maximum power transfer from harvester to the load. Maximum power transfer for the DC case occurs when the load resistance is equal to the source resistance, as shown in Figure 1.8(b) [14].

In the case of an alternating current (AC) voltage source, the load should provide a complex conjugate match to the source.

Complex conjugate matching produces the maximum small signal transfer of power from a source that is not a transmission line to a load at the sacrifice of:

- Stability (lack of self-oscillation)
- Noise
- Harmonic distortion
- Intermodulation distortion
- Temperature coefficients
- Large signal power
- Slew rate

- Large signal power conversion efficiency
- Amplitude frequency response
- Phase frequency response
- Differential group delay distortion
- Pulse fidelity
- Overload recovery
- Sensitivity to transistor production lot parameter variations

This is such a great sacrifice of performance parameters that the only time complex conjugate matching is used is when monetary costs are more important than anything else. This is usually the case when the active devices are very expensive and have low gains.

It also involves the situation where the source impedance cannot be changed. Making the source impedance complex will conjugately match the load impedance and degrade the gain by 6 dB and also reduce the large signal power conversion efficiency a further compounded 50%.

Making the phase angle of the load voltage and current equal is desirable. A complex load impedance produces an elliptical load line which produces distortion even in a totally "linear" circuit. [15].

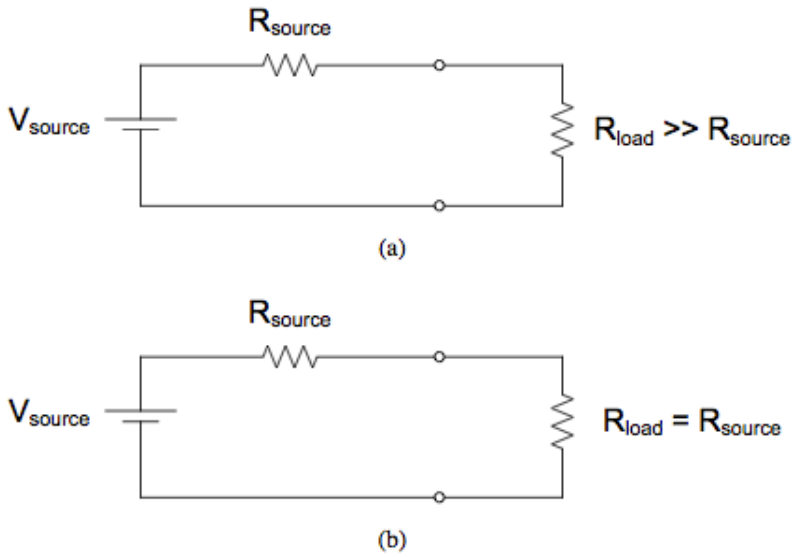


**Figure 1.8: (a) Condition for load impedance to achieve maximum efficiency of energy transfer from the source to the load, (b) condition for maximum power transfer to the load (b).**

For an energy harvesting transducer, the definition of the impedance of the source to which the load should be matched to is not generally as trivial as matching the load to a single electrical impedance. The source impedance will be dependent upon the type of energy harvester used and the conditions under which the harvester operates. In some circumstances based on harvester operating conditions, it may not be optimal to match the impedance of the load to that of the source due to other constraints. Nonetheless, in many cases, the input impedance of the interface circuit will be set to match that of the source.

### 1.2.4 Interface Electronics for Energy Harvesters

To make judicious use of the energy from transducers is requirement to interface the transducer and the load with a power management electronic.

With reference to electromagnetic microgenerator the power management electronic should poses capabilities such as:

- Rectification of the generated voltages and output voltage regulation.
- Voltage step-up capabilities.
- Emulation of a resistive load for impedance matching purposes.
- Power storage capabilities

Wang et al in [16] published a simple electrical interface for an electromagnetic harvester which consists of a step-up transformer which feeds two Schottky diodes (D1 and D2) and a capacitor (C) to acts as a storage component, as shown in Figure 1.9. The diodes are needed to rectify the AC nature of the output of the electromagnetic harvester. Due to the low transducer output voltage is stepped-up with a transformer with an appropriate turns ratio. However, it should be noted that to achieve a sufficiently large turns ratio, the transformer windings will have larger parasitic resistance and reactance. Rectification of the stepped-up voltage is achieved

by diode, D1, which conducts during one half of the AC output voltage followed by D2 in the other half.

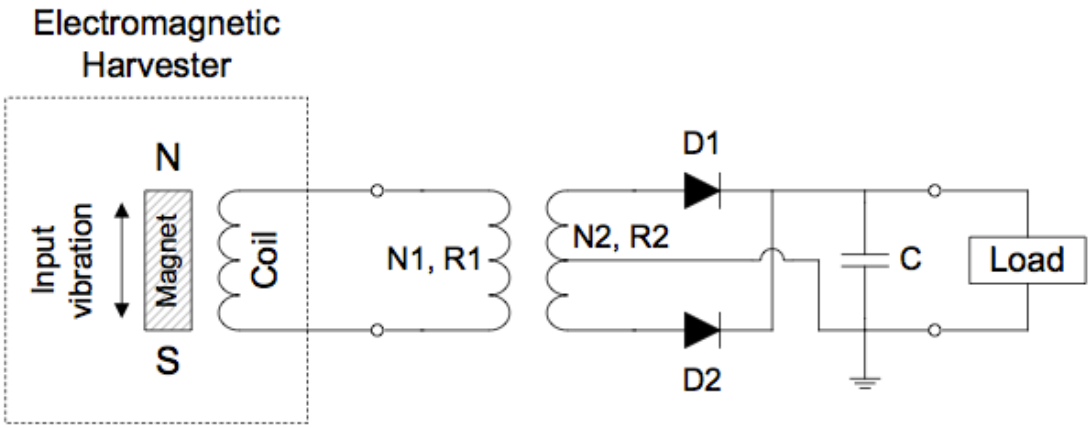


**Figure 1.9: A simple electrical interface circuit which rectifies and steps-up the voltage from an electromagnetic energy harvester, reproduced from [17].**

In the configuration shown in Figure 1.9, only one diode conducts during each half cycle of the input vibration when compared to a standard diode bridge thus minimising the effect of diode voltage drop. The simplicity of the arrangement in achieving rectification and voltage step-up is an advantage of this method.

Yan et al. in [17] employs the use of voltage multipliers such as the Villard multiplier (Figure 1.10) and the Dickson multiplier to boost voltage from the transducer. In order to achieve higher output power multiple the Villard multiplier stages are cascaded together. An advantage of this approach is that there is a reduction in component parasitic which is as a result of the absence of magnetic components. For a high voltage gain this approach will result in an increase in device size.

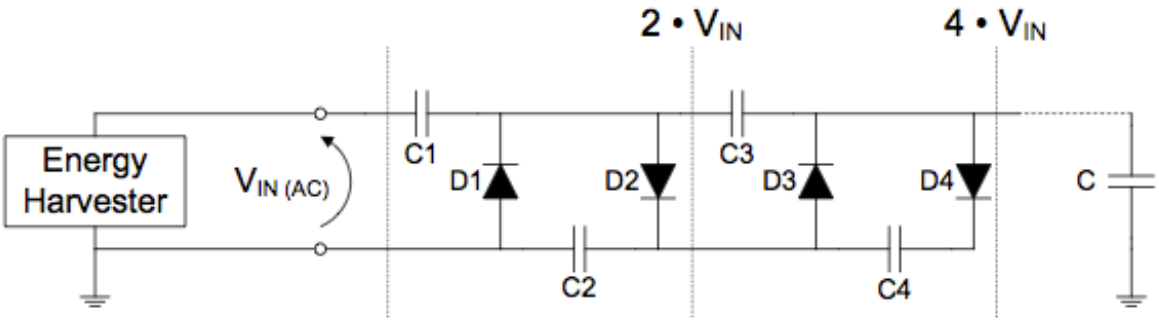


**Figure 1.10: Villard voltage multiplier for voltage up-conversion, [17].**

Mitcheson et al. published a dual-polarity boost converter to interface an electromagnetic generator.

The interface electronics was designed to provide rectification without the use of a diode bridge rectifier. The dual-polarity nature of the design provides low-voltage rectification of the positive and negative half cycles of the generated voltage.

Additionally, the circuit performs impedance matching and voltage step-up if the output voltage from the generator is inadequate to supply the interface electronics.

To reduce the effects of power loss the authors recommended the use of switched MOSFETs or Schottky diodes. The design also provided an output voltage regulation, which resulted in an output of 3.3V.

The circuit was simulated using PSPICE with a converter duty cycle of 90 % at a switching frequency of 50kHz and an input sinusoidal voltage source with a peak voltage of 95mV represented the generated voltage from an electromagnetic generator.

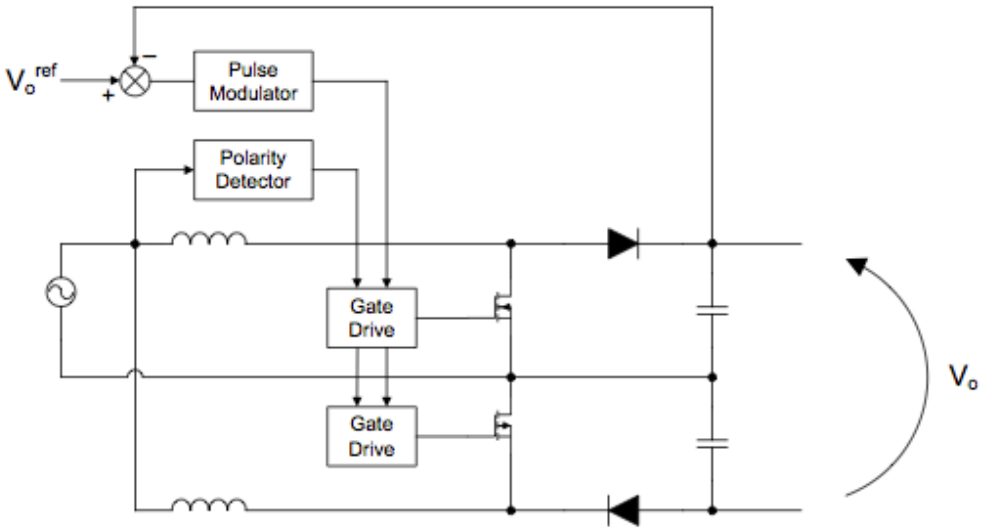


**Figure 1.11: A dual-polarity boost converter [18].**

### 1.2.5 Discussion

Reviews from on interface electronics show that as a requirement, interface electronics for an electromagnetic transducer has to perform voltage rectification and step-up because of the low AC output voltages from the harvester. Rectification was implemented using diodes and voltage step-up was achieved using either a DC/DC boost converter or a voltage multiplier. Maximum power transfer for an electromagnetic harvester requires an impedance match between the transducer and load resistances if the parasitic damping is negligible.

For work presented in this thesis, rotational energy harvesting system it is prudent to adopt few guidelines from the reviewed above such as:

- Voltage rectification is required and it is crucial that the diode voltage drop is minimized. This can be achieved by using a dual-polarity boost converter described in [18] or a transformer to lower the threshold at which the diode conducts [19].
- In the case where voltage requirement is higher than that produced from the transducer a boost converter is used to step up the transducer output voltage [20] and a buck converter is used when the transducer voltage is higher than that of the voltage required [21].
- Output voltage regulation is needed to supply a constant voltage to the load [18].

### 1.3 Problem Definition

One of the major challenges with electrically powered UAVs such as the quadcopter is endurance, thus the ability of the battery to hold flight for longer hours.

A typical quadcopter is made up of:

- Processing unit (microcontroller)
- Sensors (Gyroscope and accelerometer)
- Radio receiver
- Ground station controller (joystick, smartphone)
- Battery

- Electronic speed controllers (ESC)
- Motors

Aside these the quadcopter can carry other payloads such GPS sensor, infrared sensor, GSM module, and a camera.

The power requirement for a typical quadcopter is 3S 11.1V, 2200mAh LiPo battery.

The average flight duration of a battery powered drone with 3S 2200mAh LiPo is about 9-10minutes [4], which is very low if the drone is to be used in mission intensive application.

Most drones crash land or at worst get lost because they run out of energy while in flight, failing to achieve their purpose resulting in damage and property loss while in the middle of a mission. Therefore a means to improve its flight duration will be very beneficial to its application.

## 1.4 Research Objectives

Most of the published literatures on energy harvesters for quadcopter are either based on solar or ambient vibrations as seen in Chapter 2. These ambient solar sources are often from the sun or any high light source; vibration sources exist as a by-product of the rotating propeller, which inherently experiences continuous rotation during its operation. This thesis aims to demonstrate that rotational motion can be used directly

to harvest power for the quadcopter using BLDC generators to improve its flight duration.

The research objectives of this work includes:

1. Demonstrate a rotational energy harvester powered by rotating source using a conventional brushless direct current (BLDC) generator
2. Simulate BLDC generator using MATLAB/SIMULINK
3. Simulate and design a harvester circuit, which comprises DC-DC boost converters, using PSPICE.
4. Develop an application of harvesting rotational energy for a quadcopter.

The first research question for this work is

"Can rotational energy scavenged from the quadcopter"

The second research question is

"Can the energy harvested be used to power the quadcopter to increase its flight duration"?

### 1.5 Relevance of Research

A vertical take-off drone such as the quadcopter is a preferred choice for this research due to advantages such as it being cheap to construct, providing stable flight, ability to

carry an extensive payload including IR sensors, night vision camera etc., it is battery powered, fast and easy to control and it does not require special take-off and landing platforms.

With these advantages the quadcopter can be used in various indoor and outdoor applications such as

- Disaster monitoring and analysis (flood, fire, accidents etc.): Deployed as first responders to provide coverage or give an aerial view of to ascertain the extent of damage.
- Surveillance and reconnaissance (Ocean and border patrols): To monitor and collect data over a period of time for decision-making.
- Crime fighting: To track and monitor suspected criminals
- Reporting of industrial accidents such as oil spills and gas leaks
- Monitoring crop yield in agriculture
- Used as satellites to beam data to Earth.
- Used in academia for scientific research

With such important application improving the endurance of the quadcopter is very relevant.

This work presents a concept of quadcopter equipped with BLDC generators and power management, the setup converts rotational energy from the propellers into

electrical energy and is used to augment the primary power supply in order to improve endurance of the quadcopter.

## 1.6 Thesis Outline

The work presented in this thesis describes a rotational energy harvester for rotational motion to power a quadcopter and is organised into five chapters.

• Chapter 1 highlights the background on energy harvesting as well as the interface electronics of different types of harvesters and their applications.

Chapter 1 also discusses problem definition, project objectives and relevance of the research.

• Chapter 2 provides a literature review of the recent research on rotational harvesters and their applications for the quadcopter. An overview of the proposed work and the research scope are also presented.

• Chapter 3 discusses the system requirement, analysis and specification of the rotational harvester. The model of the rotational harvester, design consideration and selection including the developmental tools are also presented in this thesis.

• Chapter 4 presents the system simulation and experiment, implementation process, testing and results and discussion of results.

The experimental results will illustrate the capabilities of this circuit to perform output voltage regulation and energy storage.

In addition, the rectification process of the output voltage of the BLDC is also discussed.

• Chapter 5 summarises the work reported in this thesis, challenges and observations and also suggestions for future work will be discussed.

# CHAPTER 2

# LITERATURE REVIEW

## 2.1 Introduction

This chapter discusses literature review of various works, which is categorized under the following: a review on Rotational energy harvesting, characteristics BLDC generator, characteristics quadcopter and applications of energy harvesting for Drones. As part of this chapter the proposed work will be detailed as well as the scope and deliverable.

## 2.2 Rotational Energy Harvesting

The concept of rotational energy harvesting is illustrated in Figure 2.14, which describes a semi-circular mass pivoted around a central axis. The semi-circular mass allows both linear and rotational movements to produce rotating motion. The rotating mass is coupled, via a gear train, to a miniature electromagnetic generator as a transducer, which is used to charge a secondary storage device such as a battery. Such devices are described as no resonant devices. The power requirements for watches are generally very low, normally less than $1\mu W$ so the generator only needs to produce a few hundred milli-Joules each day from hand movement [2].

Non-resonant devices, allow the mass to rotate freely in either direction without any constraints on the displacement, a resonant device on the other hand requires a spring

element (and damper) to couple the mass to the frame and limit the displacement of the mass.

An example of a rotational energy transducer is Figure 2.1(b), which is also known as micro-kinetic energy generator and is made by a Netherlands company, Kinetron.

The generator is made up of a multipolar magnet that rotates inside a claw-shaped upper and lower stator. The number of claws is equal to the number of poles on the magnet. The device is similar to that used for automotive alternators. A rotating object is attached to the pinion, and the alternating voltage output is obtained from the coil.

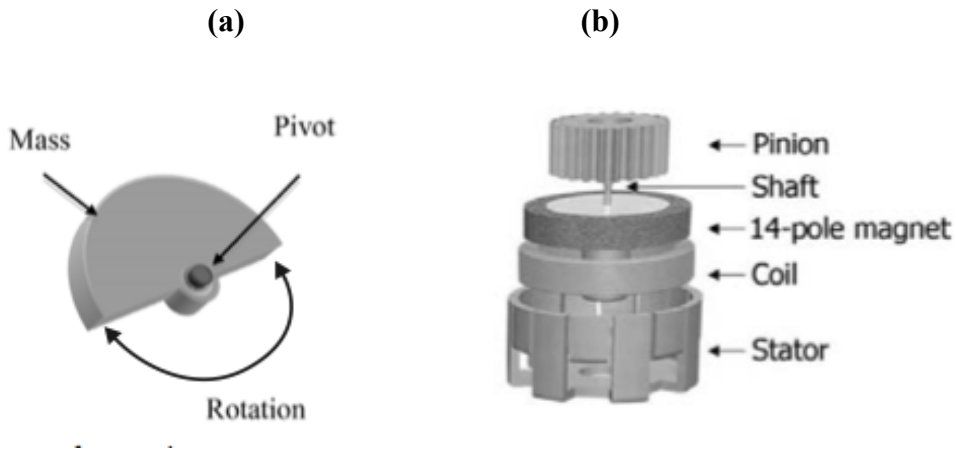


**Figure 2.1: (a) Schematic of the concept of a rotating generator as used in a self-winding watch. (b) A schematic of a multi-pole miniature rotary generator. (Courtesy of Kinetron, NL).**

Yeatman in [22] presented an analysis on energy harvesters which rely on rotating proof masses which are driven by linear or rotational motion of the host structure. Comparisons were made with inertial energy harvesters where a suspended proof mass moves linearly within the device frame when subjected to a vibrating source.

Two types of proof mass oscillatory behaviour were considered in this paper: non-resonant and resonant. In the non-resonant rotational energy harvester, the maximum output power obtainable is comparable to harvesters with a proof mass that experiences linear internal motion, which according to Mitcheson et al. in [23], is $\frac{mY_0Z_l\omega^3}{2}$ when the mass traverses an internal travel range of $Z_l$. When the non-resonant rotational device was excited by a linear vibration source, the output power is proportional to $\omega^3 Y_0$ and it is proportional to $\omega^3\Omega_0$ for excitations from a rotational source where $\Omega_0$ is maximum angular position of the device frame. In the resonant rotational device, the output power was found to scale with the mechanical quality factor of the device, which inherently will degrade the output power, once the source rotation frequency deviates from resonance. The author also proposed using a continuous rotation source, which would be coupled to the frame of a non-resonant generator and relying on gravity as a means to counteract the electrical torque from a velocity damper. This will create a difference in the angular speeds of the mass and device frame, allowing power to be extracted from the harvester.

The work by Toh in [14] uses microgenerator to harvest power from continuously rotating structures to realize a self-powered sensor on a rotating body.

Here gravitational acceleration is used instead of inertia.

The harvester is essentially a direct-current (DC) motor deployed as a generator, and it's powered directly from machine rotation, with a single point-of-attachment to the rotation source.

The rotor of a conventional electrical generator is connected to a rotational host source from which energy is being harvested. As the rotor spins, the stator is held in position by the force of gravity acting on an offset counterweight on the stator, as shown in Figure 2.2(a). As a current is drawn from the generator, the gravitational torque on the mass offset counteracts the torque between the rotor and stator, and power is generated. Another possibility for configuring the generator is shown in Figure 2.2(b), where the stator of the generator is connected to the host and the offset mass is attached to the rotor of the generator.

The DC generator is modelled as a voltage source in series with a winding resistance along with a load. To transfer power to load the electrical equivalent circuit of the generator and load is modelled as shown in Figure 2.3(a).

As current is drawn from the rotational harvester, a torque causes the proof mass to rotate such that the counter-torque from gravity, $Tg = mgLsin(\theta)$ counteracts the motor torque, $Tm = K_E I_A$ , where, $K_E$ is the motor constant and $I_A$ is the armature current in the rotor.

The $net\ torque = J_m a = T_m = K_E I_A - mgLsin(\theta)$, where $J_m$ is moment on inertia of the generator stator Figure 2.3(b).

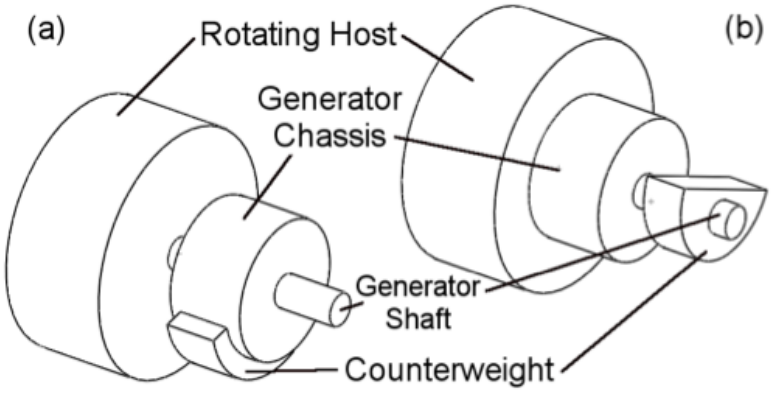


**Figure 2.2: Two possible configurations of a rotational harvester constructed from a DC motor: (a) the offset mass is attached to the stator and the rotation is coupled to the rotor, or (b) the offset mass is attached to the rotor with the rotation coupled to the stator.**

The transduction mechanism of this harvester relies on the relative speed between rotor and stator. The author also incorporated adaptive load match circuit to extract maximum power from the generator using the topology in Figure 2.4.

The primary requirement of the circuit connected to the generator is that the input impedance of the circuitry is matched to the generators armature resistance. Under matched load conditions (i.e. the output load, RL, connected to the generator is matched to the armature resistance, RA, of the generator), maximum load power can be transferred from the generator to the load. Therefore, the maximum electrical output power is given by: $P = \frac{(KE\omega)^2}{4RL}$

To realize this a switch mode power supply is connected between the generator and the load.

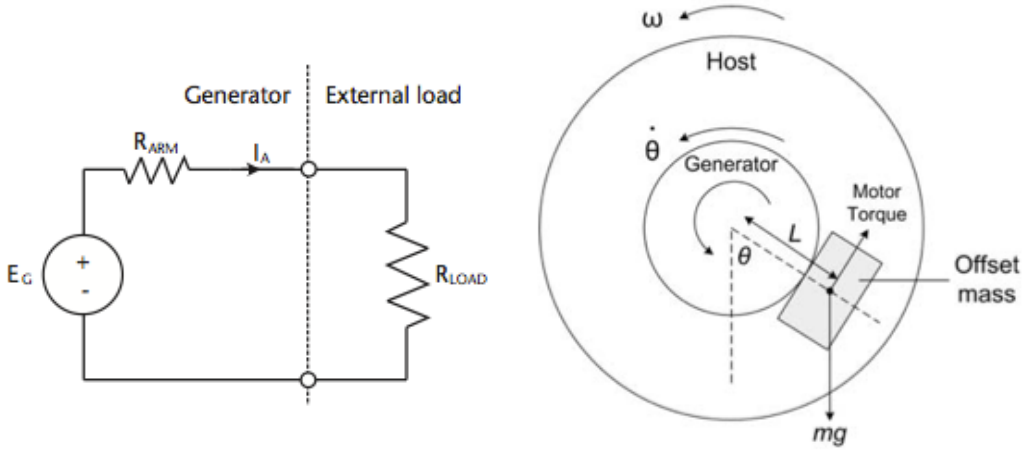


**Figure 2.3: (a) Simple DC model of the generator, (b) End view of rotational torque harvester.**

Experimental values using an on-axis setup with an offset mass of 20g produced output power levels of 1W at a source rotation speed of 8000RPM, under matched load conditions.

This work uses brushed DC motors as generator, which has a lower power density as compared to BLDC generator. Also BLDC has a longer life span and does not require maintenance.

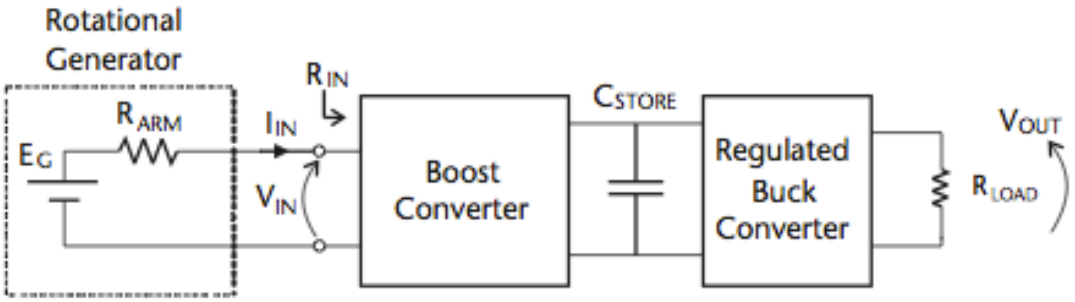


**Figure 2.4: Power processing topology for the rotational harvester.**

There has been an extensive amount of published work on kinetic energy harvesters driven by ambient vibrations from a rotating machine.

The use of vibration-driven energy harvester on rotating machinery has drawbacks as a result of the fact that the source vibrations have a fixed amplitude and frequency spectrum. Yeatman et al in [22] and Perpetuum in [24] reports that, when the vibration frequency deviates from resonance, the output power decreases, this is normal for resonant energy harvesters. For a fixed acceleration ($A = \omega^2 Y$), an increase in the source vibration frequency (ω) will cause a reduction in the source vibration amplitude (Y).

To achieve high power the machinery will have to dissipate more energy in the form of vibrations during its operation, which implies that the machine is nearing the end of its operational lifetime, thus a brand new and well-designed machine should not vibrate at all which is a disadvantage in using vibration-driven energy harvesters on rotating machinery.

According to Bartsch et al. in [25], the trajectory of the proof mass must be aligned in the direction of the source excitation and in the case of vibrations from rotating machinery, this axis is not well defined. Thus, the source vibration spectra must be obtained beforehand in order to optimally position the vibration-driven energy harvester on the host structure.

The following are advantages of vibration-driven energy harvesters on rotary machines:

• The harvester can be easily mounted on the chassis of the machine where the vibrations are prominent.

• If the harvester was designed to operate under resonance, i.e. the resonant frequency of the device matches that of the source excitation frequency, maximum power can be harvested so long as the vibration spectrum of the host structure does not change.

The disadvantages are:

• The vibrations on the rotating machinery are a by-product of the rotation and exist when the machine is not functioning properly due to misalignment of components or wear and tear of the mechanical parts. For new and well-made machines the vibration levels are low (20mg – 150mg) [26].

• the rotating machinery has to operate at a fixed speed otherwise the vibration spectrum of the host will be different to that of the vibration energy harvester.

## 2.3 Characteristics of BLDC Generator

The BLDC generator is a permanent magnet generator that has the magnets inside the machine structure. Because of the presence of a permanent magnet, the BLDC generator does not have brush and the commutator used for supplying the magnetic flux (Figure 2.5), as such maintenance for those components are not required. Joule heat from copper loss of the field winding is absent since the field winding is substituted with a permanent magnet. Also to reduce the eddy current loss the stator is laminated with steel.

The permanent magnet BLDC generator can be categorized according to the way the permanent magnets are mounted on the rotor and the shape of the induced EMF (Electromotive Force). The permanent magnets can either be surface mounted or interior mounted in the rotor, and the induced EMF shape in the stator can either be sinusoidal or trapezoidal.

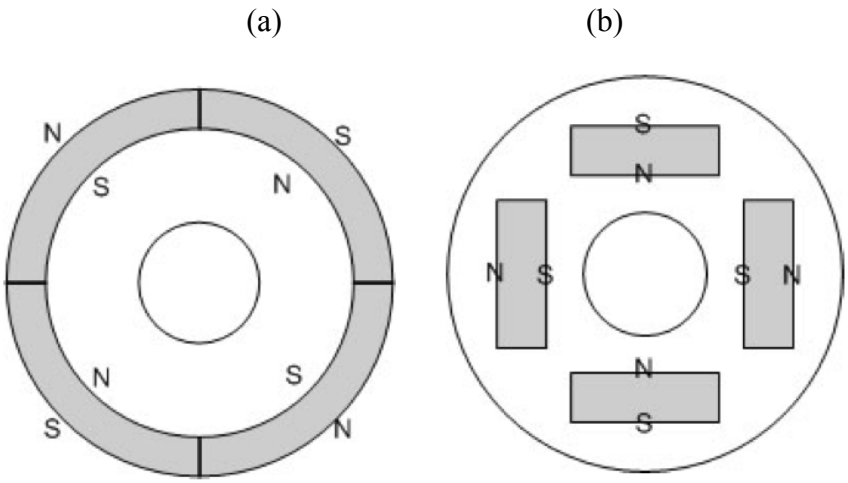


**Figure 2.5: Cross Sectional view of the permanent magnet rotors: (a) Surface-mounted PM rotor, (b) Interior-mounted PM rotor.**

In order to control electrical output power of a BLDC generator, it is essential to understand the characteristics of the induced EMF generated in the BLDC generator.

The flux linkage of a single turn coil is derived as:

$$\lambda_s = (\pi r l) B_f \left( \frac{\theta}{\frac{\pi}{2}} \right) \qquad \left( \frac{-\pi}{2} \le \theta \le \frac{\pi}{2} \right) \tag{1.1}$$

Where, $l$, $B_F$, and $\theta$ are rotor length, flux density of the permanent magnet, and rotor position, respectively. Using to Faraday's law, the induced EMF is the result of the flux crossing the airgap in a radial direction and cutting the coils of the stator at a rate proportional to the rotor speed:

$$e_s = \frac{\partial \lambda_s}{\partial t} = \frac{\partial \lambda_s}{\partial \theta} \cdot \frac{\partial \theta}{\partial t} = \frac{\pi r l B_f \omega_r}{\frac{\pi}{2}} = 2 B_f \omega_r r l \tag{1.2}$$

The magnitude of the total induced EMF with N-turn concentric windings is derived as:

$$E = 2 N_s B_f \omega_r r l \tag{1.3}$$

Where, $N_s$ is the number of turns in a phase winding.

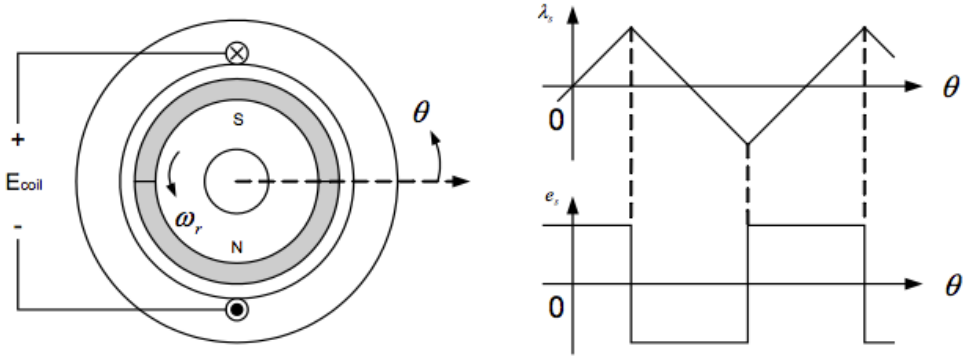


**Figure 2.6: Induced EMF waveform of a single turn coil.**

The induced EMF waveforms of three-phase stator windings are shown in Figure 2.7. The sum of EMF that is induced in an N-turn coil generates a trapezoidal waveform with a 60° electrical angle slope region created by stator winding configuration. Each phase is shifted by 120° electrical angles. The distortion of the phase EMF due to many reasons, including manufacturing imperfections (machine geometry, winding, unevenness of the surface of the permanent magnet), leakage flux, and local saturation is neglected. Therefore, the induced EMF waveform is ideally trapezoidal.

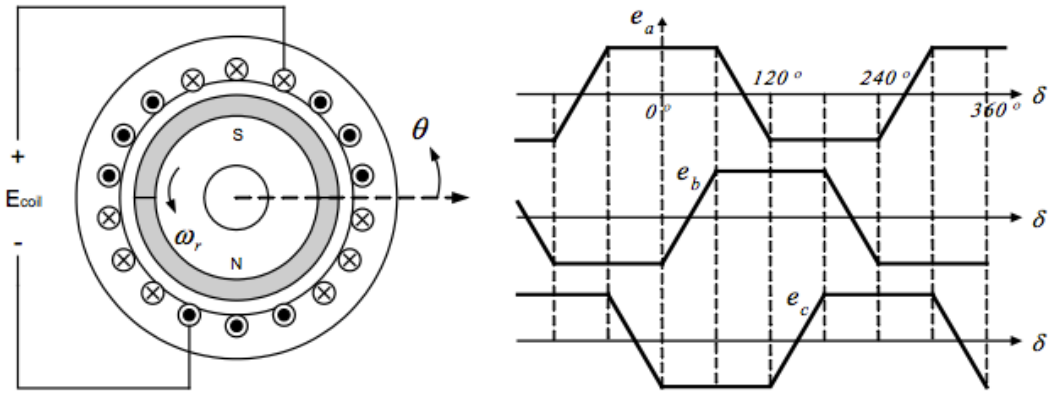


**Figure 2.7: Induced EMF waveforms of three-phase stator windings reproduced from [1].**

### 2.3.1 Advantages and Disadvantages of BLDC Generator

The BLDC generator offers many advantages such as:

• High efficiency: The BLDC machine is the most efficient of all electric machines since it has a magnetic source inside itself. Use of permanent magnets for the excitation consumes no extra electrical power. Therefore, copper loss of the exciter does not exist and the absence of mechanical commutator and brushes or slip ring means low mechanical friction losses.

• Compactness: The recent introduction of high-energy density magnets (rare-earth magnets) has allowed achievement of very high flux densities in the BLDC generator. And winding of the rotor is not required. These in turn allow the generator to be small, light and rugged structure.

• Ease of cooling: There is no current circulation in the rotor for magnetic field. Therefore, the rotor of a BLDC generator does not heat up. The only heat production is on the stator, which is easier to cool than the rotor because it is static and on the periphery of the generator.

• Low maintenance, great longevity, and reliability: The absence of brushes, mechanical commutators and slip rings suppresses the need for associated regular maintenance and suppresses the risk of failure associated with these elements. The longevity refers only to the winding insulation, bearing, and magnet life- length. Low

noise: There is no noise associated with the mechanical contact. The driving converter switching frequency is high enough so that the harmonics are not audible.

Also, the BLDC generator has some inherent disadvantages such as:

• Cost: Permanent magnets are expensive parts in the machine and result in an increased motor cost. The cost of higher energy density magnets prohibits their use in applications where initial cost is a major concern.

• Limited operating-speed range: The field-weakening operation for the BLDC machine is somewhat difficult due to the use of permanent magnets. Some accidental speed increase might damage the power electronic components above the rating of converter, especially for vehicle applications. In addition, the surface-mounted permanent magnet generators cannot reach high speeds because of the limited mechanical strength of the assembly between the rotor yoke and the permanent magnets. There is a possibility of permanent magnets to fly apart.

• Demagnetization of the permanent magnet: Magnets can be demagnetized by large opposing magneto-motive-force (MMF) and high temperatures. The critical demagnetization force is different for each magnet material. Extreme care must be taken to cool the generator, especially if it is compact [28-29].

## 2.4 Structure of Quadcopter [28]

A quadcopter is an electrically powered helicopter with four rotors. Because of its unique design comparing to traditional helicopters, it allows a more stable platform, has the ability to hover, and take-off vertically making quadcopters ideal for many indoor and outdoor tasks and allows it to be operated in nearly any environments.

Unlike a helicopter, a quadrotor has four rotors all work together to produce upward thrust and each rotor lifts only 1/4 of the weight, so we can use less powerful and therefore cheaper motors. Varying the relative thrusts of each rotor controls the quadcopter's movement.

These rotors are aligned in a square, two on opposite sides of the square rotate in clockwise direction and the other two rotate in the opposite direction Figure 2.8(a). If all rotors turn in the same direction, the craft would spin just like the regular helicopter without tail rotor.

(a) (b)

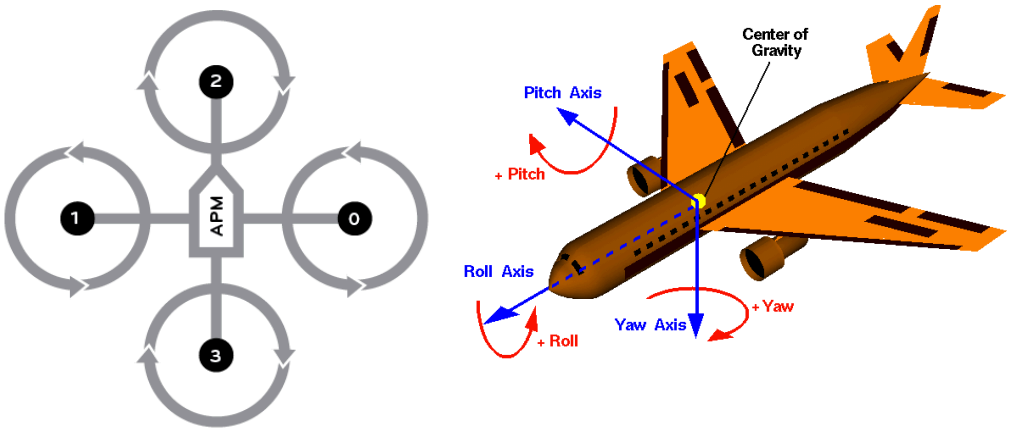


**Figure 2.8: (a) Quadcopter structure, (b) degrees of freedom [29]**

The aerodynamic torque of the first rotors pair cancelled out with the torque created by the second pair which rotates in the opposite direction, so if all four rotors apply equal thrust the quadcopter will stay in the same direction.

To maintain balance, the quadcopter must be continuously taking measurements from the sensors, and making adjustments to the speed of each rotor to keep the body level. Usually these adjustments are done autonomously by a sophisticated control system on the quadcopter in order to stay perfectly balanced. A quadcopter has four controllable degrees of freedom: Yaw, Roll, Pitch, and Altitude as in Figure 2.8(b). Adjusting the thrusts of each rotor can control each degree of freedom.

- Yaw (turning left and right) is controlled by turning up the speed of the regular rotating motors and taking away power from the counter rotating; by taking away the same amount that you put in on the regular rotors produce no extra lift (it won't go higher) but since the counter torque is now less, the quadrotor rotates and control becomes a matter of which motor gets more power and which one gets less.
- Roll (tilting left and right) is controlled by increasing speed on one motor and lowering on the opposite one.
- Pitch (moving up and down, similar to nodding) is controlled the same way as roll, but using the second set of motors. Roll and pitch are determined from

where the "front" of the quadrotor is, and in a quadrotor they are basically interchangeable and mostly determined by the onboard sensors.

To roll or pitch, one rotor's thrust is decreased and the opposite rotor's thrust is increased by the same amount. This causes the quadcopter to tilt. When the quadcopter tilts, the force vector is split into a horizontal component and a vertical component. This causes two things to happen: First, the quadcopter will begin to travel opposite the direction of the newly created horizontal component. Second, because the force vector has been split, the vertical component will be smaller, causing the quadcopter to begin to fall. In order to keep the quadcopter from falling, the thrust of each rotor must then be increased to compensate.

Using accelerometers the angle of the quadcopter in terms of X, Y, and Z axes is measure and accordingly adjust the RPM (Revolutions per Minute) of each rotor in order to stabilize itself.

All sensors are connected to a microcontroller, which coordinate and make the decision as to how to control the motors.

This design provides an inherent level of stability while the on-board accelerometers, gyroscope and other electronics work to keep it level and also provide commands that it needs to fly.

The following are essential components needed to develop a quadcopter:

- Frame – The structure that holds all the components together. The designed has to compromise between strength and weight.
- Rotors – Brushless DC motors that can provide the necessary thrust to propel the craft. ESC (Electronic Speed Controller) – Each rotor needs to be controlled separately by an ESC.
- Propeller
- Battery – Power Source
- IMU (Inertial Measurement Unit) – Sensors
- Microcontroller – The Brain
- Flight controller

### 2.4.1 Quadcopter Frame

Frame is the structure that holds all the components together, the frame is designed to be strong, rigid, and be able to absorb the vibrations from the motors as much as possible. The common materials used for the frame are carbon fiber, aluminium and wood, such as plywood. The structure is composed of a center plate where the electronics are mounted and four arms mounted to the center plate, a motor is mounted at the end of each arm.

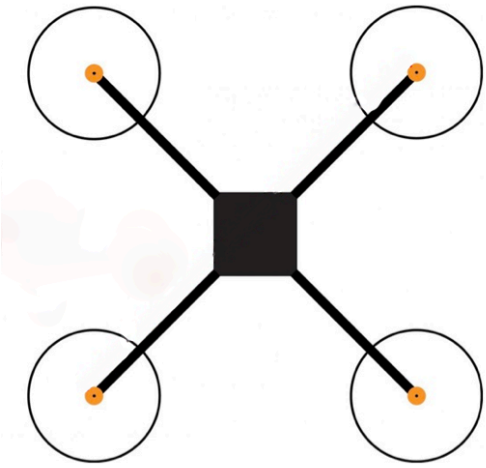

**Figure 2.9: Quadcopter frame**

### 2.4.2 Brushless Motors

They are a built to use electromagnetic principles using coils and magnets to drive a shaft. Similar to normal DC motors brushless motors do not have a brush on the shaft which takes care of switching the power direction in the coils, this is why they are called brushless.

Brushless motors come in many different varieties, with different sizes and the current consumption. Brushless motors are specified by their "KV-rating". The KV-rating indicates how many RPMs (Revolutions per minute) the motor will do when provided with a number of volts. Generally brushless motors spin in much higher speed and use less power at the same speed than DC motors. Also brushless motors don't lose power in the brush-transition like the DC motors do, so it's more energy efficient.

### 2.4.3 Propellers

Each brushless motor has a propeller mounted on it. Two of the propellers together with the motors rotate in the opposite directions to the other two to avoid body spinning. By making the propeller pairs spin in each direction, but also having opposite tilting, all of them will provide lifting thrust without spinning in the same direction. This makes it possible for the quadcopter to stabilize.

### 2.4.4 ESC (Electronic Speed Controller)

The brushless motors are multi-phased, normally 3 phases, so direct supply of DC power will not turn the motors on. That is where the Electronic Speed Controllers (ESC) comes into play. The ESC generating three high frequency signals with different but controllable phases continually to keep the motor turning. The ESC is also able to source a lot of current as the motors can draw a lot of power. Each ESC is controlled independently by a PPM signal (similar to PWM). The frequency of the signals also vary a lot, but for a quadcopter it is recommended the controller should support high enough frequency signal, so the motor speeds can be adjusted quick enough for optimal stability (i.e. at least 200Hz or even better 300Hz PPM signal).

### 2.4.5 Battery

Typically the power source of the quadcopter is a LiPo Battery, this battery is a recommended choice because it is light and current ratings meets the current requirement of the quadcopter as compared to other battery types. LiPo battery can exist as a single battery pack of over 10 cells connected in series each rated 3.7V.

A popular choice of battery for a quadcopter is the 3SP1 batteries which means three cells connected in series as one battery, which should give us 11.1V.

To determine the battery capacity for a particular application, the following needs to be determined:

- Total power that motors will draw.
- Flight duration required.
- How much weight the battery will contribute to total weight.

Battery discharge rate is specified by the C-value. The C-value together with the battery capacity indicates how much current can be drawn from the battery.

## 2.5 Applications of Energy Harvesting in Electrically Powered UAV

In the above sections various energy-harvesting methods have been reviewed and among the methods it's evident that solar energy has the most power density with respect to outdoor applications on a bright day.

As such various researches have sorted to solar energy harvesting as a means to prolong the endurance on small electrically powered UAV's.

The first ever quadcopter which relies solely on solar energy has been reported by [30]. Seven postgraduate students at Queen Mary University of London built a solar powered quadcopter, which they dubbed "Solar Copter".

While there have been numerous solar-powered aircraft, this is the first ever solar powered quadcopter. Based around a unique frame design you can see a lot of potential for surveillance, search and rescue, and long-term deployments in areas of the world where the sun shines a lot. This implementation will not be efficient if considered for an indoor application or used in areas where there is little sunshine.

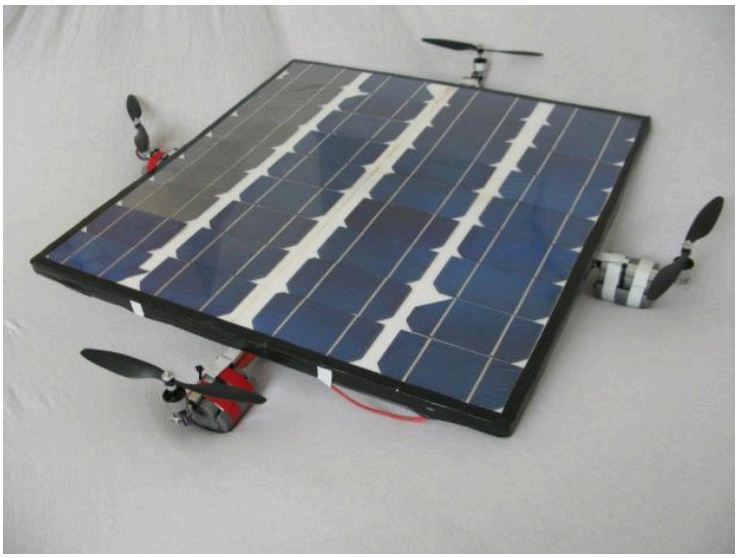

**Figure 2.10: Worlds first solar quadcopter [30].**

Grady [31] reports of a lightweight, solar-powered drone dubbed, Zephyr's with a massive 73-foot wingspan which flew above the clouds for 14 days.

Built by British defence contractor QinetiQ, the drone's 336 hour, 22 minute and 8 seconds marked the longest time an airplane flew without refuelling.

With such tremendous endurance success companies like Google and Facebook has both acquired solar drone manufacturing companies to build drone satellites equipped with laser to beam Internet to underdeveloped countries.

Likewise this work will have challenges if it used for an indoor applications since illumination is not that high making solar harvester inefficient.

**Figure 2.11: The Zephyr by QinetiQ [31].**

A novel concept is presented by Anton in [32] involving the combination of piezoelectric devices and new thin-film battery technology to form multifunctional self-charging, load- bearing energy harvesting devices for use in UAV systems. The proposed self-charging structures contain both power generation and energy storage

capabilities in a multilayered, composite platform consisting of active piezoceramic layers for scavenging energy, with thin- film battery layers for storing scavenged energy and a central metallic substrate layer. The compact nature of the devices allows easier integration into UAV systems and their flexibility provides the ability to carry load as structural members. A potential application of the self- charging structures is use in the wing spars of UAVs or as the entire wing of an MAV.

The interface circuit for the harvester contains a full wave diode rectifier, a smoothing capacitor, and a Texas Instruments TPS71501 adjustable output voltage regulator as reproduces in Figure 2.12(a).

It has been found that continuous power on the order of at least 10μW can be generated during flight of an RC glider aircraft from piezoelectric fiber-based devices mounted at the root of the wings.

In this work, vibration energy was harvested for a fixed-wing UAV which is capable for only outdoor applications.

Anton in [33] presented a hybrid approach to energy harvesting from both aircraft vibrations and ambient sunlight for a mini UAV specifically a remote controlled (RC) glider aircraft with a 1.8 m wing span

The RC glider was modified to include two piezoelectric patches (MFC and PFC) placed at the roots of the wings and a PFC cantilevered piezoelectric beam installed in

(a) (b)

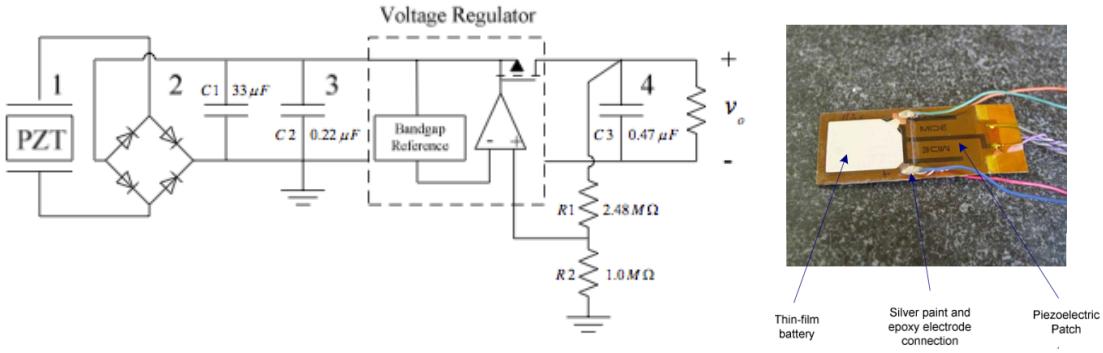


**Figure 2.12: (a) Energy harvesting circuit, (b) Complete self-charging device.**

the fuselage to harvest energy from wing vibrations and rigid body motions of the aircraft, as well as two thin film photovoltaic panels attached to the top of the wings to harvest energy from sunlight, specifically "PowerFilm RC7.2-75" PSA panels.

The EasyGlider is a completely foam aircraft with an electric propulsion system composed of an electric motor and an 11.1V, 2100mAh Lithium Polymer battery.

During flight, the aerodynamic loading on the wings of the aircraft will cause the wings to vibrate. As the wings deflect, the piezoelectric patches mounted on the wing spar will be strained and thus create energy. The cantilever PFC inside the fuselage of the aircraft will harvest energy when the plane moves rigidly in the vertical direction. Such motions are typical in a small UAV aircraft as the wings are loaded aerodynamically and as the plane flies through non-homogenous air pockets. When the plane moves up and down, the effects of inertia on the tip mass will cause the beam to oscillate. The oscillations will cause strain in the beam and thus generate

energy. Oscillatory motion of all three piezoelectric devices when excited will cause an alternating voltage output.

The outputs of the three piezoelectric patches would be wired together in parallel, in order to increase the current output, and connected to the input of an EH300 energy-harvesting chip from Advanced Linear Devices.

The average power output of the cantilever PFC, the MFC attached and the PFC both attached to the wing spar were found to be 24.0μW, 11.3μW, and 10.1μW, respectively. Though hybridization improves the power density for the UAV, therefore improving the endurance, this UAV can only be used for outdoor applications.

## 2.6 The Proposed Work

The work reported in this thesis converts ambient continuous rotational motion from the rotors of a quadcopter to usable electrical power using a microgenerator, instead of harvesting vibrational energy from rotating machines or using brushed DC generator to harvest rotational motion.

An interface electronic circuit of the harvester is used to conditions the electrical energy harvested from the rotation, the final output of the harvester is used to augment the power supply of the quadcopter in order to increase its flight duration.

Typically, the immediate interface to an energy harvester is a rectifier stage, a voltage step-up stage after which the output voltage is regulated across a load

## 2.7 Research Scope

The main goal of the work presented in this thesis is to prove the concept of harvesting rotational energy from a quadcopter to prolong its duration. This goal is achieved by the following deliverables.

### 2.7.1 Deliverables

- Simulation of BLDC microgenerator
- Simulation and Prototype of harvester circuit
- Test prototype of an electrically powered quadcopter

# CHAPTER 3

# METHODOLOGY

## 3.1 Introduction

This chapter presents the design concept of harvesting energy for quadcopter. The development process and mathematical model of the BLDC microgenerator are presented. System requirements and analysis are also discussed.

## 3.2 System Design Problem and Process

Rotational motion can be converted into electricity by using an electromagnetic generator as a transduction mechanism. Functionally the rotor of the generator is driven by a prime mover and the stator of the generator is bolted to the stationary. When current flows in the generator, a torque on the rotor acts to reduce the velocity of the prime mover which in turn causes a torque on the stator, which coincidentally is prevented from moving due to its fastenings.

In light of the work undertaken in this project, which is to harvest energy from the rotors of the quadcopter to extend its energy supply, the rotational energy harvester should have two attachment points. The prime mover being the rotor of the quadcopter has its stator fastened to the quadcopter frame to make it stationary and on the other hand the generator's stator is also fastened to make it stationary, Figure 3.1.

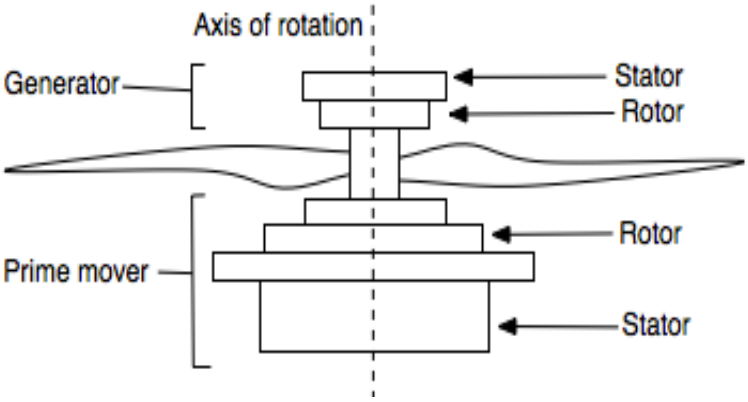


**Figure 3.1: Implementation of the rotational harvester: the prime mover is coupled to the generator shaft.**

To achieve the transduction process of converting rotational energy to electrical energy, an electromagnetic microgenerator is used. The output of the microgenerator is rectified due to the AC nature of the output to obtain a DC voltage. Based on the power requirement of the quadcopter, a DC-DC boost converter is used to step-up the output of the rectifier. The output of the boost converter is used to boost the power supply of the quadcopter and also charge the battery if enough energy is produced, Figure 3.2.

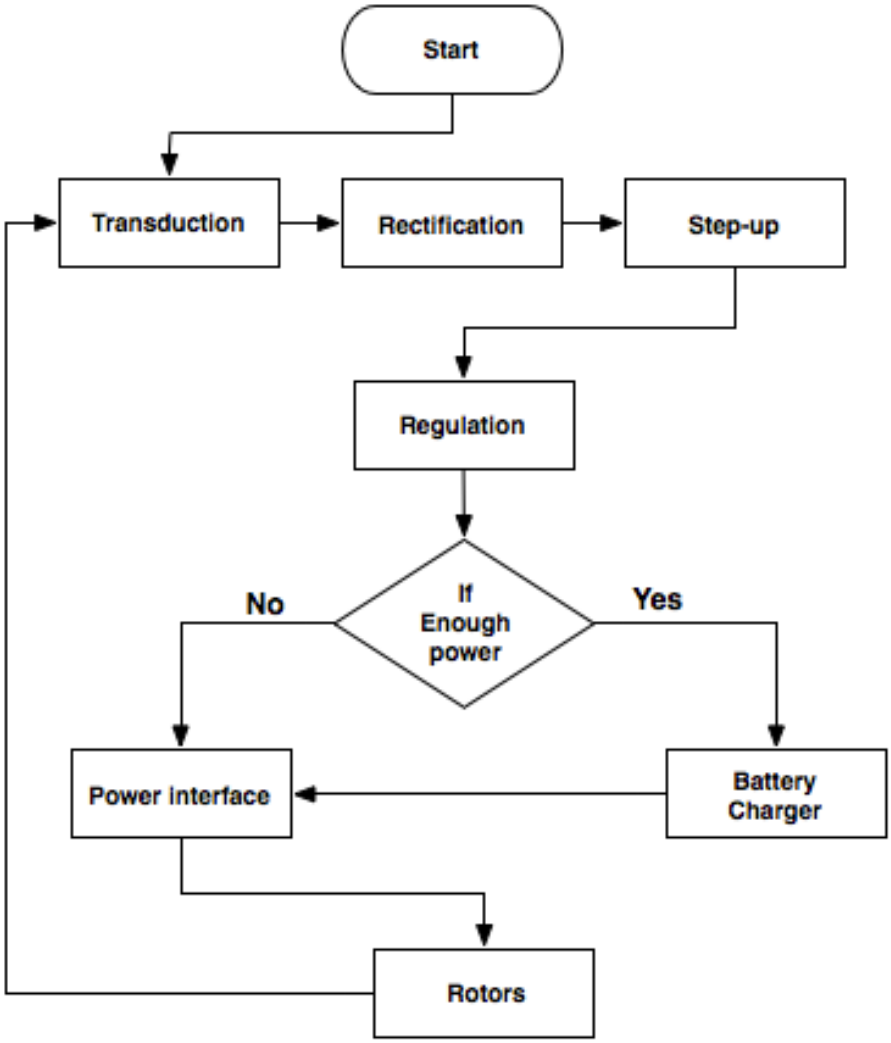


**Figure 3.2: Design Process flowchart.**

### 3.2.1 BLDC Generator Model

When dealing with rotational motion, it is preferable to use torque instead of force to analyse the mechanical behaviour of the bodies in question.

The terminals of the generator is connected to a three-phase bridge rectifier circuit, the output of all the four generators are connected in parallel, this connection is done to sum up the current produced from each generator.

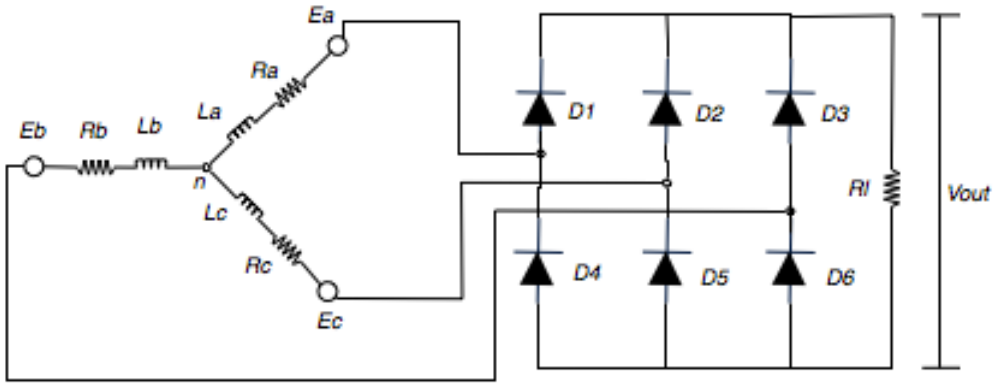


**Figure 3.3: Equivalent circuit of the BLDC generator.**

Figure 3.3 shows the equivalent circuit of the BLDC generator. The analysis is based on the following assumptions for simplification:

- The generator is operated within the rated condition, so the generator is not saturated.
- Stator resistance and inductance of all the windings are equal. All three phases have an identical induced EMF shape.
- Iron losses are negligible.

As presented in [34], [35] and [1] , by using Kirchhoff laws, phase voltage equations of the BLDC generator can be expressed as:

$$\begin{aligned} e_{an} &= R_a i_a + \frac{\partial\left(L_{aa}(\theta,i_a)\,i_a + L_{ab}(\theta,i_b)\,i_b + L_{ac}(\theta,i_c)\,i_c\right)}{\partial t} + v_{an} \\ e_{bn} &= R_b i_b + \frac{\partial\left(L_{ba}(\theta,i_a)\,i_a + L_{bb}(\theta,i_b)\,i_b + L_{bc}(\theta,i_c)\,i_c\right)}{\partial t} + v_{bn} \\ e_{cn} &= R_c i_c + \frac{\partial\left(L_{ca}(\theta,i_a)\,i_a + L_{cb}(\theta,i_b)\,i_b + L_{cc}(\theta,i_c)\,i_c\right)}{\partial t} + v_{cn} \end{aligned} \tag{3.1}$$

Based on the assumptions:

$$\begin{aligned} &R_a = R_b = R_c = R \\ &L_{aa} = L_{bb} = L_{cc} = L_s \\ &L_{ba} = L_{ab} = L_{ca} = L_{ac} = L_{bc} = L_{cb} = L_m \\ &L_s = L_m = L \\ &i_a + i_b + i_c = 0 \end{aligned} \tag{3.2}$$

Equation (3.2) can be represented as:

$$\begin{aligned} ean &= Ria + \left(Ls - Lm\right)\frac{\partial ia}{\partial t} + van = Ria + L\frac{\partial ia}{\partial t} + van \\ ebn &= Rib + \left(Ls - Lm\right)\frac{\partial ib}{\partial t} + vbn = Rib + L\frac{\partial ib}{\partial t} + vbn \\ ecn &= Ric + \left(Ls - Lm\right)\frac{\partial ic}{\partial t} + vcn = Ric + L\frac{\partial ic}{\partial t} + vcn \end{aligned} \tag{3.3}$$

Equation 3.3 can be simplified as:

$$e_{xn} = Ri_x + L\frac{\partial i_x}{\partial t} + v_{xn} \tag{3.4}$$

Where, $e_{xn}$, $v_{xn}$, $i_x$, $R$, $L$, $L_s$ and $L_m$ represent each phase EMF, each phase-to-neutral voltage, each phase current, phase resistance, inductance, self-inductance, and mutual

inductance, respectively. EMF calculation can be accomplished by sensing each phase current ($i_x$) and voltage ($v_{xn}$). And motion equation can be represented as:

$$\begin{aligned} T_{rotor} &= T_{generator} + B\omega_r + J\frac{\partial \omega_r}{\partial t} \\ \frac{\partial \omega_r}{\partial t} &= \frac{1}{J}\left(T_{rotor} - T_{generator} - B\omega_r\right) \end{aligned} \tag{3.5}$$

Where, B and J represent viscous friction and inertia.

The back-emf and electrical torque ($T_e$) can be expressed as:

$$T_e = \frac{1}{\omega_r}\left(e_a i_a + e_b i_b + e_c i_c\right) \tag{3.6}$$

$$\begin{aligned} e_a &= \frac{k_e}{2}\omega_r F\left(\theta_e\right) \\ e_b &= \frac{k_e}{2}\omega_r F\left(\theta_e - \frac{2\pi}{3}\right) \\ e_c &= \frac{k_e}{2}\omega_r F\left(\theta_e - \frac{4\pi}{3}\right) \end{aligned} \tag{3.7}$$

$$Te = \frac{kt}{2}\left[F\left(\theta_e\right)i_a + F\left(\theta_e - \frac{2\pi}{3}\right)i_b + F\left(\theta_e - \frac{4\pi}{3}\right)i_c\right] \tag{3.8}$$

where $k_e$ and $k_t$ are the back-emf constants and torque constant respectively. The electrical angle $\theta_e$ is equal to the rotor angle times the number of poles pairs ($\theta_e = p\theta_m$). One period of the trapezoidal waveform of the back-emf is given by:

$$F(\theta_e)=\begin{cases} 1, & 0 \le \theta_e < \dfrac{2\pi}{3} \\ 1-\dfrac{6}{\pi}\left(\theta_e-\dfrac{2\pi}{3}\right), & \dfrac{2\pi}{3} \le \theta_e < \pi \\ -1, & \pi \le \theta_e < \dfrac{5\pi}{3} \\ -1+\dfrac{6}{\pi}\left(\theta_e-\dfrac{5\pi}{3}\right), & \dfrac{5\pi}{3} \le \theta_e < 2\pi \end{cases}, \quad (3.9)$$

One important characteristic of the BLDC generator is its efficiency; to compute efficiency of the generator the formula 3.10 is used.

$$\eta = \frac{Pout}{Pin} \times 100 \quad (3.10)$$

$$P_{out} = i_a v_a + i_b v_b + i_c v_c \quad (3.11)$$

$$P_{in} = \frac{1}{2} J \omega r^2 + \omega_r T_{generator} \quad (3.12)$$

### 3.3 System Requirements, Analysis and Specifications

The aim of the design process is to achieve an efficient power system.

To achieve the design process in the above section the following requirements need to be satisfied:

- Rotational transduction
- Low power rectification
- DC-DC boost converter
- Power regulation

- LiPo battery charger

With the aim of converting ambient rotational energy to electrical energy the rotational transducer is coupled with the rotor of the quadcopter. With this setup rotational energy is converted to electrical energy based on electromagnetic principles. The output of the microgenerator is rectified and stepped-up using the DC-DC boost converter, which gives an output of 18VDC base on the power requirement of the quadcopter. To ensure a stable voltage supply to the quadcopter and other electronic payloads the output of the DC-DC boost converter is regulated. The LiPo battery charger is required to charge the 3s LiPo battery of the quadcopter whilst it's in flight.

### 3.4 Design Considerations and Selection

The system design approach presented in this thesis is geared towards enhancing the flight duration of the quadcopter for both indoor and outdoor applications.

From chapter two it was presented that solar is the best choice when it comes to outdoor application of drone, this is because of the abundance of light during the day and also the fact that solar has the best power density when compare to other energy harvesting technique such as vibrating energy harvesting. Unfortunately for indoor applications solar harvester will perform poorly due to inadequate light. In such situation, vibration energy harvesting is resorted to as a means to boost endurance.

From the design of the quadcopter it has more ambient rotational energy than linear vibrational energy, therefore the choice to harvest energy using micro-electromagnetic generator instead of piezoelectric vibration harvester. The specific microgenerator used in this work is the BLDC generator which has more advantages than its DC counterparts as seen in chapter two. A low voltage three phase bridge rectifier is achieved using Schottky diode for the rectification process, this selection is made to reduce the voltage drop by the diodes and also to keep the design simple.

Because the rotation on the quadcopter is dynamic thus the RPM of each rotor is varied in order to cause motion, the output voltage of the generators vary, this means the design choice for the step-up converter should be one with low volts boost and should also allow a wide range of input voltage. The choice of a two stage boost is made firstly to boost and condition the wide range and low input voltage to a higher voltage, secondly to boost the output of the first boost converter to a much higher voltage with regulation and high current capabilities. The choice to design a charger with a balancing circuit is made to charge the 3s LiPo battery of the quadcopter.

These design considerations are made in order to achieve the purpose of harvesting rotational energy to augment the power supply of quadcopters.

## 3.5 System Design

A quadcopter is a helicopter with four (4) rotors, to harvest energy to prolong its duration the system architecture in Figure 3.4 is employed.

From Figure 3.4 the rotors of the quadcopter are each coupled with BLDC microgenerator generators. The ground pilot control is used to control the flight of the quadcopter thus to arm or spin the rotors.

As the rotor or the quadcopter spins torque is transferred to the coupled generator which causes the rotor of the generator to spin, the torque of the generator opposes the torque generated from the quadcopter rotor and the difference in these torques causes power to be generated. For a BLDC generator the generated voltage is a trapezoidal alternating current (AC) in 3 phase, therefore the generated voltage is rectified to produce a direct current (DC) voltage using a 3 phase bridge rectifier. The produced DC Voltage is fed into a power management circuit to power and charge the quadcopter battery where necessary.

Figure 3.5 describes a simplified topology of the energy harvesting system.

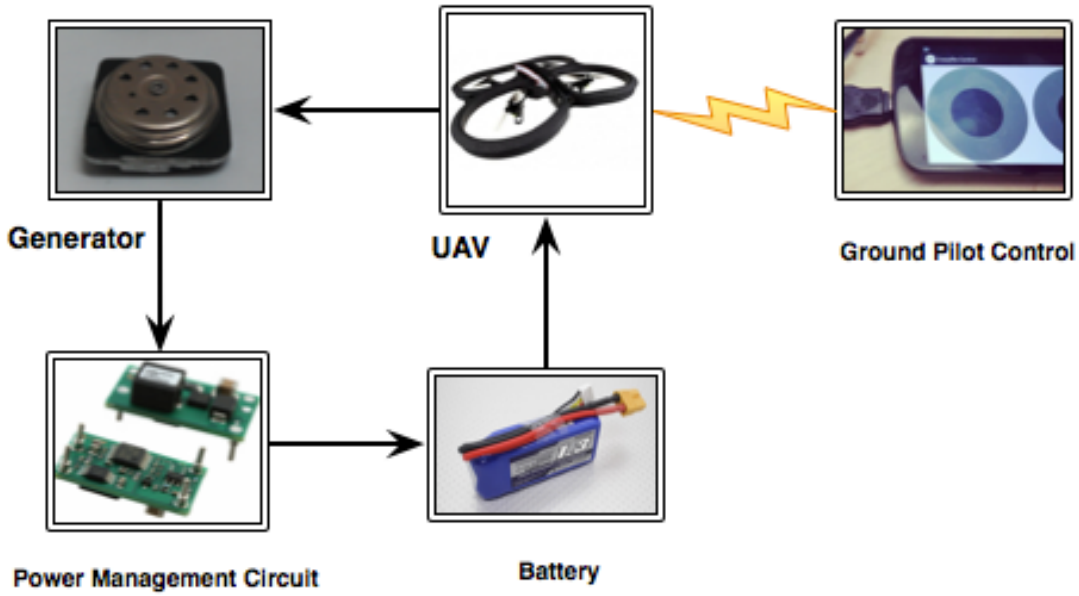


**Figure 3.4: System Architecture.**

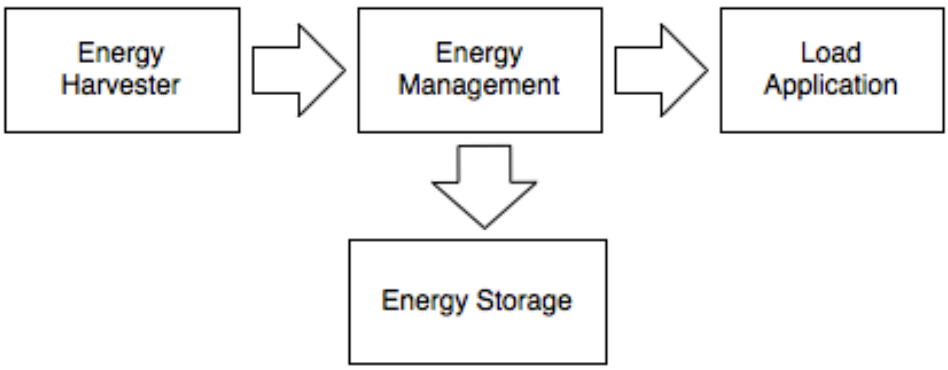


**Figure 3.5: Simplified Electrical System Architecture.**

## 3.6 Development Tools

Table 3.1 and Table 3.2 show a list of software and hardware developmental tools used in this work to accomplish the objectives.

**Table 3.1: Software development tools**

| |
|---|
| Matlab R2012a® |
| Arduino 1.0.5 |
| Eclipse JUNO |
| Cadsoft Eagle 6.4.0 |
| Cadence PSPICE 16.3 |

**Table 3.2: Hardware development tools**

| **Tools** | **Quantity** |
|---|---|
| SMD rework station | 1 |
| SMD components | |
| Resistor | - |
| Capacitor | - |
| Inductor | - |
| Transistor | - |
| Trimmer | - |
| TPS | 1 |
| BQ25504 | 1 |
| Turnigy BESC programming card | 1 |
| 5.4x4.3 Propeller (Standard and counter clockwise) | 6 |
| Turnigy Plush 10 amp speed controller | 4 |
| Rhino 750mAh LiPo Pack | 2 |
| Power supply | 1 |
| 1.5V battery | 1 |
| See Appendix B for full hardware list | |

# CHAPTER 4

# SYSTEM IMPLEMENTATION AND TESTING

## 4.1 Introduction

This chapter discusses the system implementation process, which encompasses the rectification process of the harvester output, power management circuit and charging of the quadcopter battery.

Discussion of results and performance evaluation is also presented.

## 4.2 System Implementation Process

The physical model of the BLDC generator is implemented using motors obtained from 5.4" HDD. The BLDC generators are coupled directly to each of the rotors on the quadcopter and care is taken to align the rotors axis of rotation to that of the generator. Because the generator is light in weight and has less friction the effects of friction are ignored, thus torque is applied directly from the rotor to the generator.

As the rotor of the generator rotates, its torque oppose the torque generated from the rotation source and the difference in these torques will cause power to be generated, which can then be dissipated onto a load. In this setup the counter-torque is provided by anchoring the generator's chassis (stator) to a non-rotating structure, while the rotor is coupled to the rotation source.

### 4.2.1 MATLAB /SIMULINK Simulation of BLDC Microgenerator

This section presents MATLAB / SIMULINK implementation of the BLDC generator. The parameter of the generator was obtained partly from datasheet and partly from measured values. Table 4.1 shows generator parameters.

The simulation was done in MATLAB R2012a® and SIMULINK 8 using the default ode45 Solver. The simulation time was 0.1 seconds and a load torque of $0.00875\ Nm$ was applied. Figure 4.1 shows a complete BLDC generator Simulink model. The core block implements equations (3.3-3.12). As Figure 4.2 shows, the mechanical block takes in as input the rotor torque ($T_r$) and the electrical torque ($T_e$) and gives out angular velocity ($\omega_r$) as output. The trapezoidal signals are calculated using the electrical angle as input signals, Figure 4.3. The electrical block set takes as input $\omega_r$ and trapezoidal signal with a phase load of $100k\Omega$ to produce the phase emfs and subsequently the phase voltages and currents as shown in Figure 4.2. The phase currents in conjunction with the trapezoidal signals and the generator tongue constant produce the electrical torque.

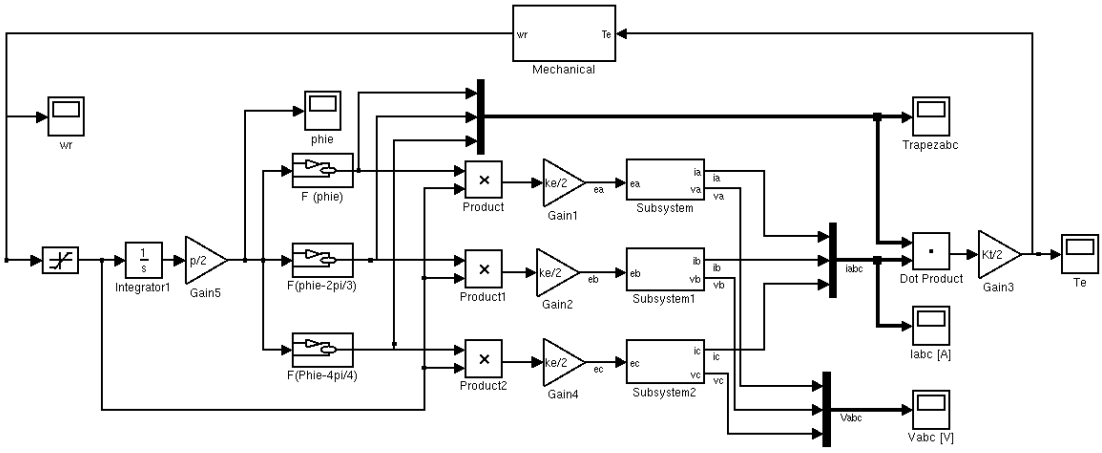


**Figure 4.1: The BLDC generator model.**

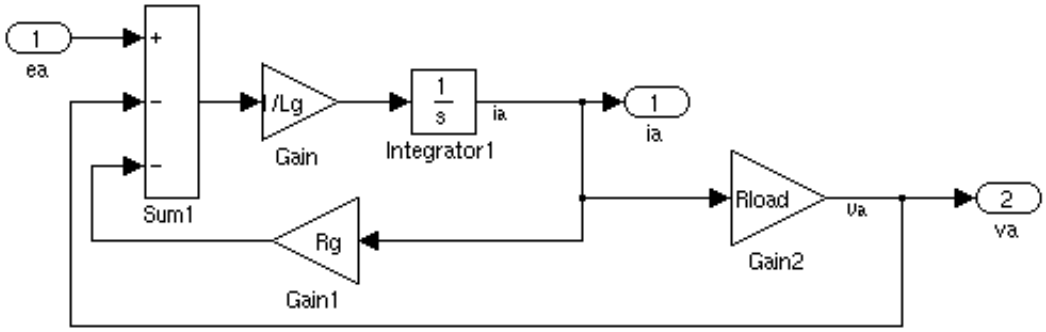


**Figure 4.2: Electrical subsystem: Phase a. (Similar for phases b and c).**

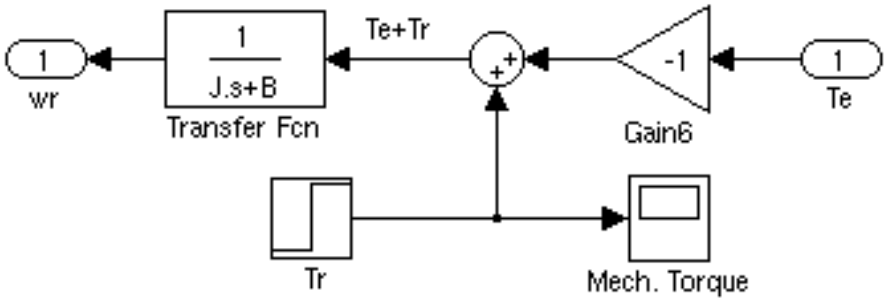


**Figure 4.3: Torque and angular velocity calculation.**

(a) (b)

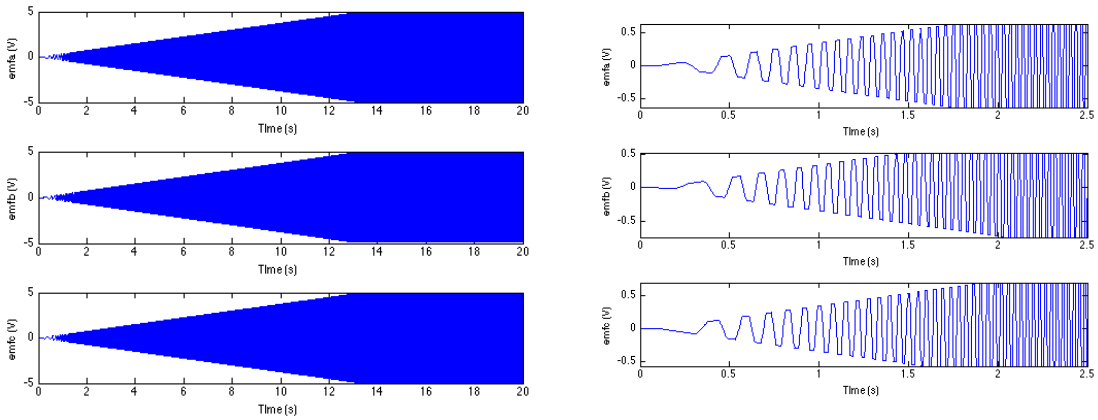


**Figure 4.4: (a) Simulink results: EMF (b) Zoomed in.**

(a) (b)

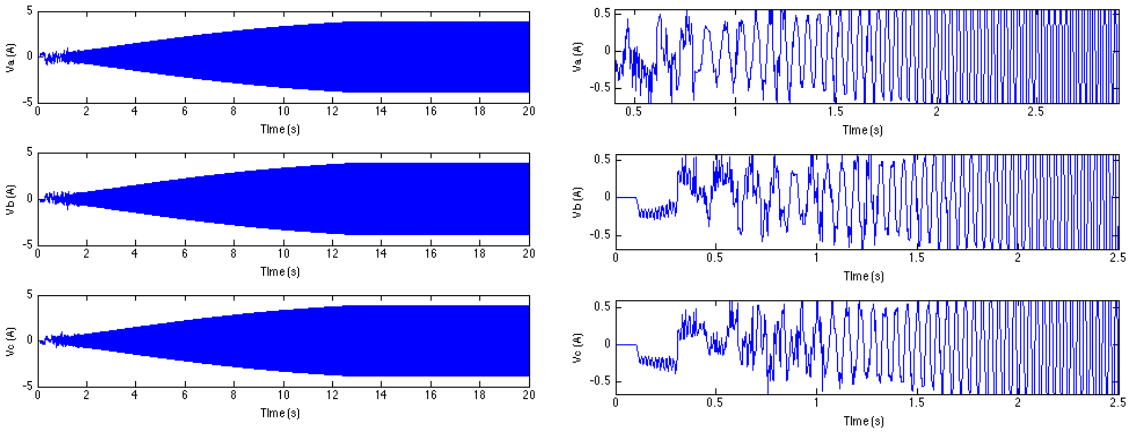


**Figure 4.5: (a) Simulink results: Voltage (b) Zoomed in.**

(a) (b)

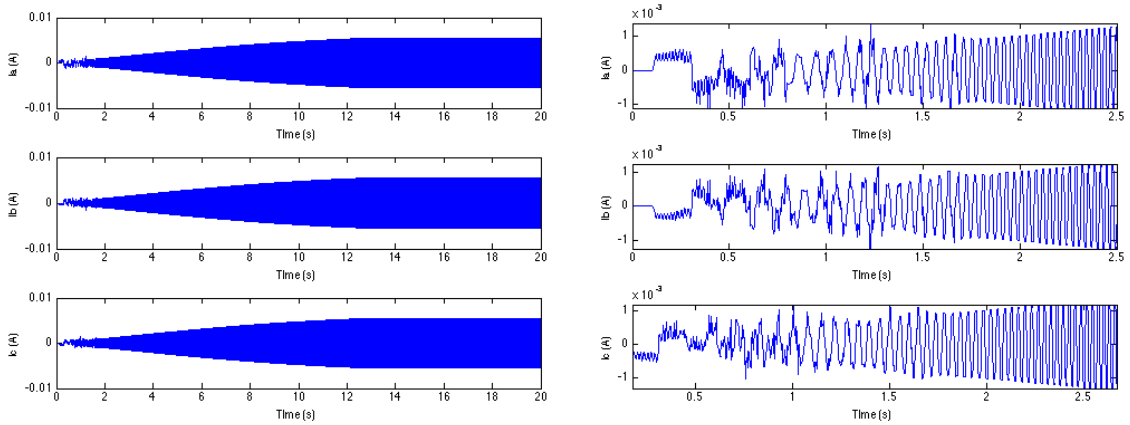


**Figure 4.6: (a) Simulink results: Current (b) Zoomed in.**

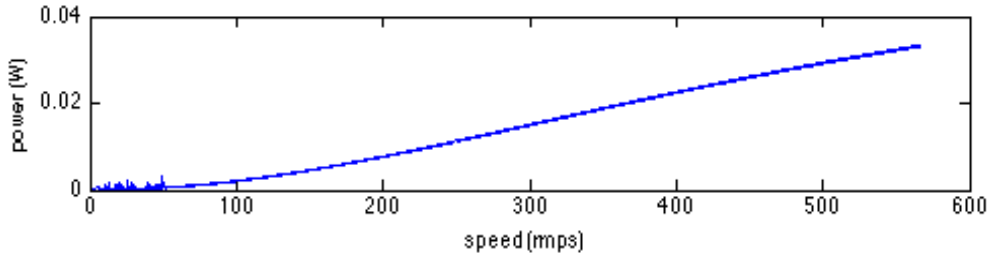


**Figure 4.7: (a) Simulink results: Power Vs. RPM**

The generator parameters used in the modelling are summarised in Table 4.2.

The graph in Figure 4.4 shows the trapezoidal nature of the back EMF of the generator, it begins gradually from 0 to about 5V. Figure 4.5 and Figure 4.6 are the graphs for voltage and current respectively, the current starts gradually from 0 to about 0.5A while the voltage starts from 0 to 4.3V, in both cases this occur as the generators speed increase from 0RPM to 5400RPM. Figure 4.7 is a graph of power output versus generator speed in RPM. Table 4.1 gives a summary of the results.

**Table 4.1 Simulation results at maximum revolution**

| Parameter | Value |
|---|---|
| Voltage | 4.3 |
| Current | 0.5A |
| Power | 2.15W |

### 4.2.2 Initial Experiment

An initial experiment was conducted to find the generator parameters such as EMF constant Ke and inductance L.

#### 4.2.2.1 EMF Constant (Ke)

To determine Ke a rotation source was coupled to the generator's rotor and the open circuit output voltage measured. Figure 4.8 shows a plot of the open circuit voltage against the rotation speed; the gradient of the graph gives Ke (Line-to-line) for this generator.

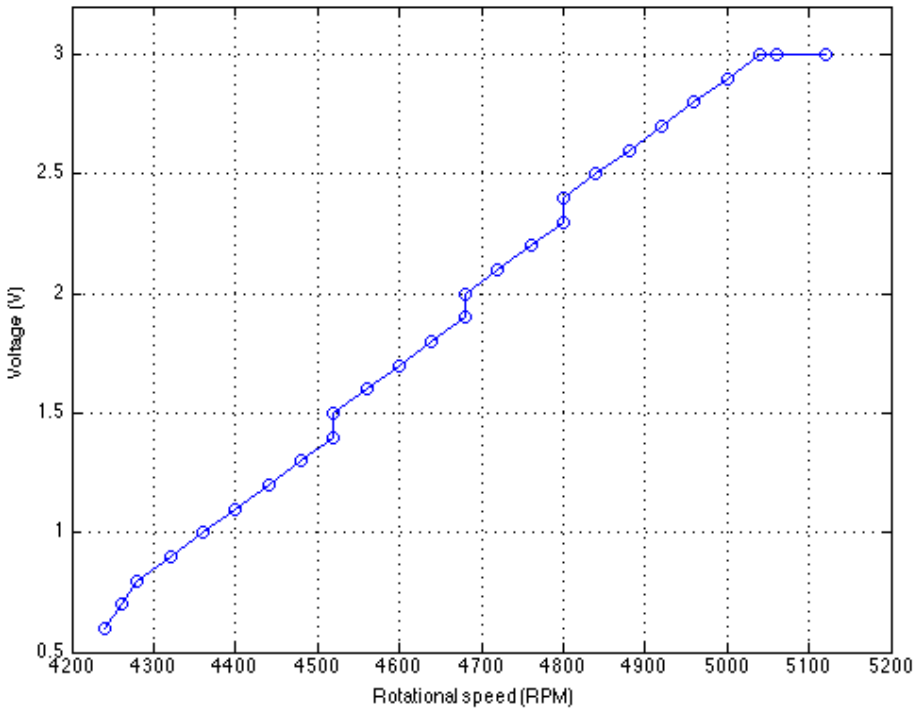


**Figure 4.8: Plot of voltage against RPM.**

To obtained Ke for each phase, Ke (Line-to-line) is divided by √3=1.73.

The Ke (phase) was calculated as 0.01724.

#### 4.2.2.2 Inductance (L)

To measure the generator inductance a low voltage AC source is applied to one pair of the three phase wires of the generator. The voltage and the current are measured using a multimeter, the readings obtained are line-to-line to phase values, and the line-to-line values are divided by √3. The impedance of the generators phase winding is then obtained using:

$$Z = \frac{v_x}{i_{xy}} \tag{4.1}$$

$$Z = \sqrt{X^2 + R^2}$$
$$X = \sqrt{Z^2 - R^2} \tag{4.2}$$

Where Z, $v_x$ and $i_{xy}$ are impedance, phase voltage and line-to-ling current respectively.

The impedance is calculated as 2.508325Ω and the reactance is calculated using equation 4.3 as 0.2042Ω. The value for resistance is obtained using a multimeter as: 2.50Ω.

The inductance can then be calculated using;

$$X = 2\pi fL$$
$$L = \frac{X}{2\pi f} \tag{4.3}$$

The frequency ($f$) of the AC source is 50Hz.

The results for the generator parameters from the experiment are found in Table 4.2.

**Table 4.2 Parameters of the BLDC generator**

| Phase voltage ($V_x$) | Value | Units |
|---|---|---|
| Current ($I$) | 0.55 | A |
| Resistance ($R$) | 2.5 | Ω |
| Voltage ($V$) | 5 | V |
| Revolution ($R$) | 5400 | RPM |
| Torque Constant ($K_L$) | 0.00540 | Nm/A |
| EMF constant ($K_e$) | 0.01724 | V/rad/s |
| Inductance ($L$) | 0.65 | mH |

### 4.2.3 Rectification of the BLDC generator [17]

In chapter 2, characteristics of the BLDC generator were described and it was presented that the BLDC generator is a non-sinusoidal AC (Alternating Current) power supply system, instead it has a trapezoidal output waveforms. PM (Permanent Magnet) generators such as BLDC generators are used for small rated power supply

systems because of the PM, therefore using an AC-to-DC converter between the BLDC generator and load equipment is essential. In this section, the rectification method for AC-to-DC conversion in described.

In most power electronics applications, a simple full-bridge diode rectifier is used for the AC-to-DC conversion. Its advantages are:

- Simple construction: A full-bridge diode rectifier has six diodes in one package as in Figure 4.9. No additional hardware is required.
- No control: The diode is a passive element in the power electronics. There is no control to conduct circuits.
- Low cost

This method of rectification is adopted in this thesis for simplicity and also to proof the concept of rotational energy harvesting for quadcopter.

Figure 3.3 shows the equivalent circuit of the BLDC generator with a diode rectifier. The rectified electrical power is connected to the load as a DC voltage source.

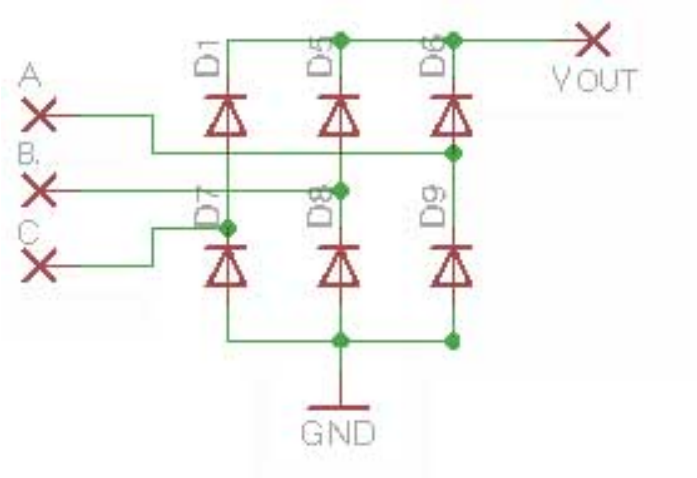


**Figure 4.9: Full bridge diode rectifier circuit**

### 4.2.4 DC-DC Boost Converter

In order to meet the requirement to power the quadcopter and charge the 11.1V battery at 1.5A, the 2.5V generated from the BLDC generator needs to be stepped-up and regulated. To achieve the 11.1V requirement two boost converters are employed to step up the generated voltage. The first boost converter steps up the 2.5V to 5.2 at a maximum of 0.2A, which is then fed to the second boost converter. The second boost converter steps up the 5.2V to 18V, which is used as an input to a LiPo charger to charge and power the quadcopter as in Figure 4.10.

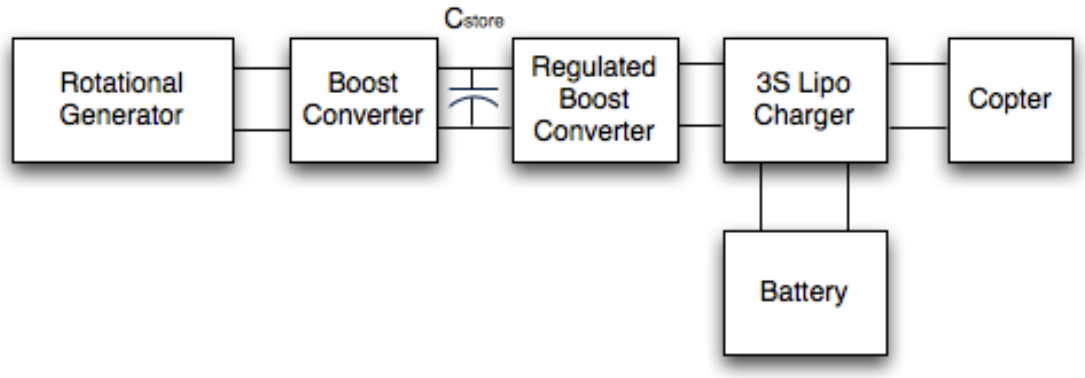


**Figure 4.10: Topology of rotational harvester circuit.**

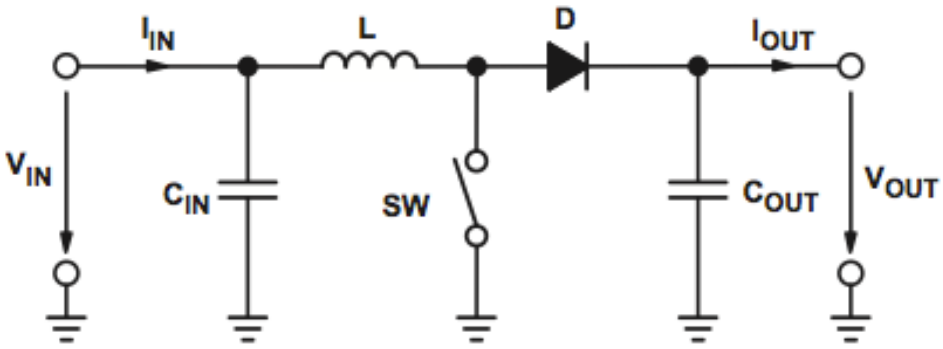


**Figure 4.11: Boost converter power stage.**

Figure 4.11 shows the basic configuration of a boost converter where the switching part is done in an IC (integrated Circuit).

When the switch is conducting, current flows through the inductor and the inductor stores energy by creating a magnetic field, causing the left side of the inductor to be positive. When the switch stops conducting, current flow is limited as impedance is higher and the magnetic field previously created is destroyed to maintain the current flow towards the load. Thus reversing polarity of the inductor. As a result two sources (Vin and the inductor) will be in series causing a higher voltage to charge the capacitor through the diode D.

If the switch is cycled fast enough, the inductor will not discharge fully in between charging stages, and the load will always see a voltage greater than that of Vin when the switch is conducting. Also while the switch is conducting, the capacitor in parallel with the load is charged with the combined voltage. When the switch stops conducting the capacitor is therefore able to provide the voltage and energy to the load, during this time, the blocking diode prevents the capacitor from discharging through the switch. It is not advisable for the capacitor to discharge to zero because of this the switch is cycle fast to prevent this condition.

#### 4.2.4.1 5.2v Boost Converter Design

The Texas TI BQ25504 IC is used to generate the pulse frequency modulation (PFM) cycle which is used to control the switch on the boost converter. Details of the IC can be found in its datasheet in the Appendix.

BQ25504 is an ultra-low power, high efficiency dc/dc boost converter/charger with battery management. The choice for this IC was made because the design starts with a DC-DC boost converter/charger that requires only microwatts of power to begin operating, it has less number of external components needed for its implementation and it's designed for energy harvesting.

The boost converter is used to step up the voltage from rectifier circuit to 5.2V.

The BQ25504 priority is to charge up the $V_{STOR}$ capacitor, $C_{STOR}$, then power additional internal circuitry via $V_{STOR}$ or $V_{\mathrm{BAT}}$ with the energy available from the DC input source. For the first 32 ms after the main converter is turned ON, the charger is disabled to let the input go up to its open-circuit voltage. This is needed to get the reference voltage which will be used for the remainder of the charger operation till the next MPPT sampling cycle turns ON. The boost converter employs pulse frequency modulation (PFM) mode of control to regulate the input voltage (VIN_DC) close to the desired reference voltage. Input voltage regulation is obtained by transferring charge from the input to VSTOR only when the input voltage is higher than the voltage on pin VREF_SAMP. The current through the inductor is controlled through internal current sense circuitry. The peak current in the inductor is dithered internally to set levels to maintain high efficiency of the converter across a wide input current range. The converter nominally transfers up to an average of 100mA of input current.

To prevent damage to storage element, both maximum and minimum voltages are monitored against the user programmed undervoltage (UV) and overvoltage (OV) levels.

The boost converter is disabled when the voltage on $V_{\mathrm{STOR}}$ reaches the OV condition to protect the battery connected at VBAT from overcharging.

Table 4.3 outlines the specifications for the boost converter.

**Table 4.3 Boost converter (BQ25504) parameters**

| | | Value | Unit |
|---|---|---|---|
| $V_{IN}$ | DC input voltage into $V_{IN\_DC}$ | 0.3 - 3 | V |
| $V_{OUT}$ | DC output voltage at $V_{STORE}$ | 5.25 | V |
| $V_{OV}$ | Over Voltage –Sets maximum output voltage | 5.20 | V |
| $V_{UV}$ | Under voltage setting for shorting $V_{STORE}$ to VBAT | 3.20 | V |
| $V_{BAT\_OK}$ | $V_{BAT\_OK}$ indication toggles high when VSTOR ramps up | 3.50 | V |
| | $V_{BAT\_OK}$ indication toggles low when $V_{STORE}$ ramps down | 3.20 | V |

Because BQ25504 incorporates a battery charger, requirements such as overvoltage, undervoltage, batteryok for charging a battery needs to be set.

To ensure the correct operation of the boost converter the external components must be carefully selected and calculated.

For the BQ25504 to operate properly, an inductor of appropriate value must be connected between Pin 16 ($L_{BST}$) and Pin 2 ($V_{IN\_DC}$) for the boost converter.

For the boost converter and or charger, the inductor must have an inductance = 22µH and have a peak current capability of ≥250mA with the minimum series resistance to keep high efficiency as recommended by the manufacturer.

Energy from the energy harvester input source is initially stored on a capacitor $C_{\mathrm{HVR}}$ tied to Pin 2 ($V_{IN\_DC}$) and ground ($V_{SS}$, Pin 1) for this configuration an initial value of 4.7 µF is recommended by the manufacturer.

Operation of the BQ25504 requires two capacitors to be connected between Pin 15 ($V_{\mathrm{STOR}}$) and ground. A high frequency bypass capacitor of 0.01µF should be placed as close as possible between VSTOR and GND. In addition, a bulk capacitor of at least 4.7µF should be connected between Pin 15 and ground to assure stability of the boost converter [36].

Battery undervoltage threshold is set to prevent rechargeable batteries from being deeply discharged and damaged, and to prevent completely depleting charge from a capacitive storage element. This protection measure is set using external resistors. The VBAT_UV threshold voltage when the battery voltage is decreasing is given by

$$V_{BAT\_UV} = V_{BIAS}\left(1+\frac{R_{UV2}}{R_{UV1}}\right) \tag{4.4}$$

The sum of the resistors, $R_{UV1}\ and\ R_{UV2}$ should be $10M\Omega$, $V_{BIAS}$ is a voltage node which is used as reference for the programmable threshold voltage, $V_{BIAS} = 1.25$.

Battery overvoltage threshold is set to prevent rechargeable batteries from being exposed to excessive charging voltages and to prevent over charging a capacitive storage element. This protection measure is set using external resistors and is given by

$$V_{BAT\_OV} = \frac{3}{2} V_{BIAS} \left( 1 + \frac{R_{OV2}}{R_{OV1}} \right) \tag{4.5}$$

The sum of the resistors, $R_{OV1}$ $and$ $R_{OV2}$ should be $10M\Omega$.

The IC allows the user to set a programmable voltage independent of the overvoltage and undervoltage settings to indicate whether the VSTOR voltage is at an acceptable level, equation 4.6 set the threshold when the battery voltage is decreasing.

$$V_{BAT\_OK\_PROG} = V_{BIAS} \left( 1 + \frac{R_{OK2}}{R_{OK1}} \right) \tag{4.6}$$

Equation 4.7 sets the threshold when the battery voltage is increasing.

$$V_{BAT\_OK\_HYST} = V_{BIAS} \left( 1 + \frac{R_{OK2} + R_{OV2}}{R_{OK1}} \right) \tag{4.7}$$

#### 4.2.4.2 PSPICE Implementation of BQ25504

The boost converter circuit implemented in PSPICE is shown as in Figure 4.12.

The transient simulation model of the BQ25504 resulted in the graphs presented in Figure 4.13.

### 4.2.5 18V Boost Converter design

To meet the power requirement for the quadcopter a second boost converter was implemented to boost the 5.2V of the first boost converter to 18V at a maximum of 2A in order to power and charge the quadcopter battery.

**Table 4.4 BQ25504 external components values**

| | |
|---|---|
| $L_{BST}$ | $22\mu H$ |
| $C_{\mathrm{HVR}}$ | $4.7\mu F$ |
| $V_{\mathrm{STOR}}$ | $4.7\mu F$ |
| $R_{OV1}$ | $3.52M\Omega$ |
| $R_{OV2}$ | $6.48M\Omega$ |
| $R_{UV1}$ | $6.12M\Omega$ |
| $R_{UV2}$ | $4.83M\Omega$ |
| $R_{OK1}$ | $3.32M\Omega$ |
| $R_{OK2}$ | $6.12M\Omega$ |
| $R_{OK3}$ | $5.42K\Omega$ |

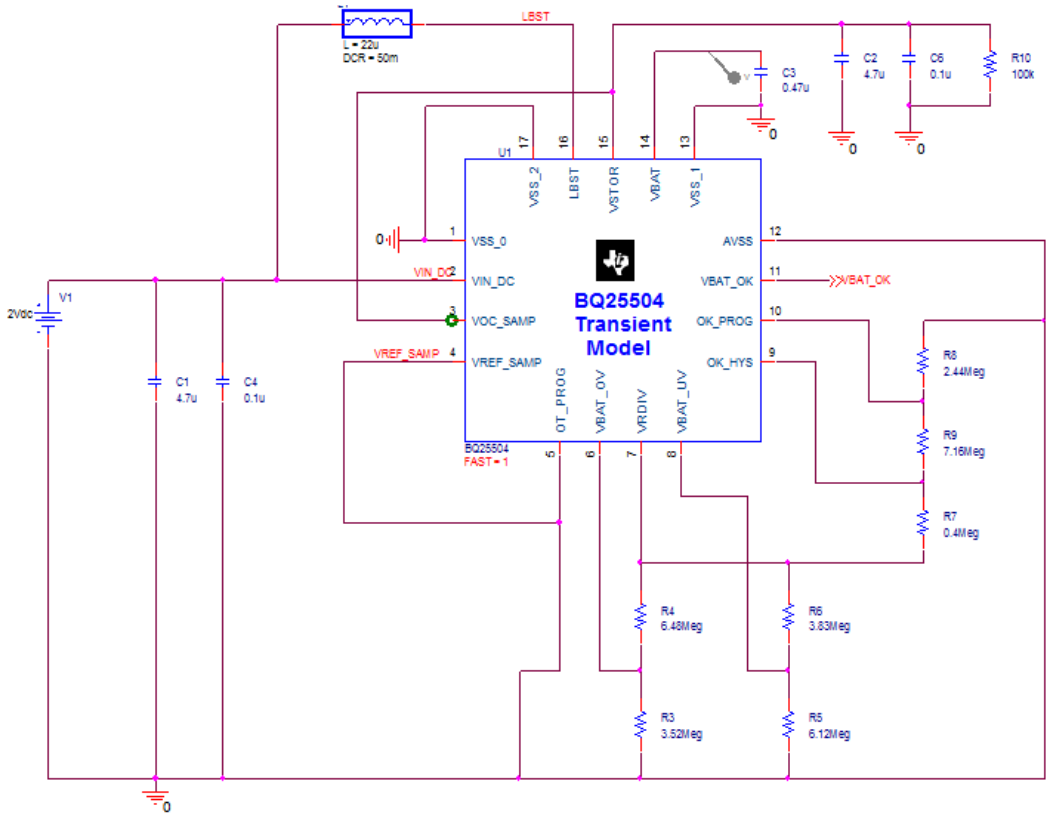


**Figure 4.12: PSPICE Simulation circuit (BQ25504).**

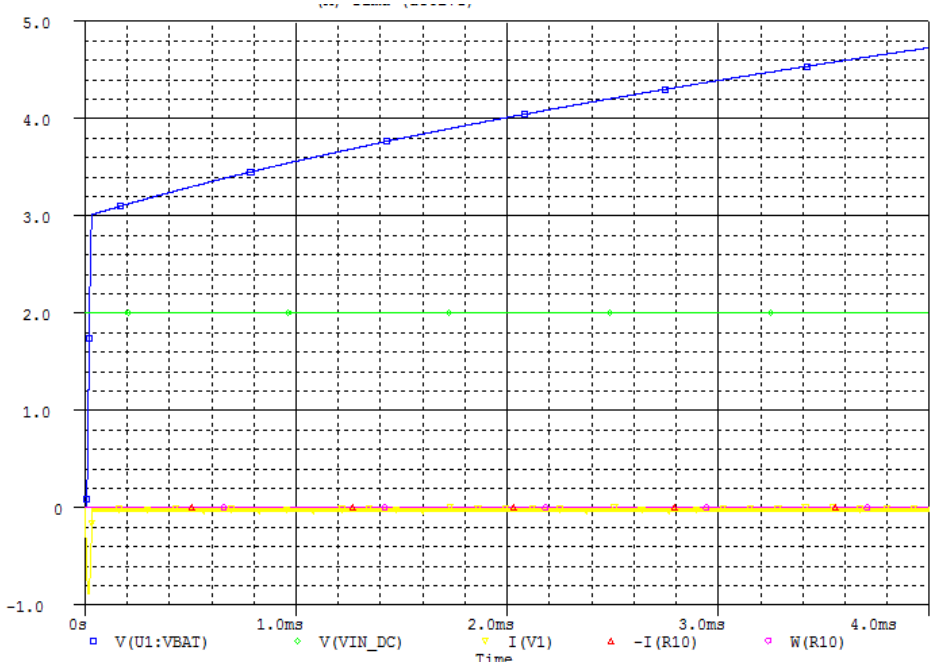


**Figure 4.13: PSPICE Simulation results (BQ25504).**

The IC TPS55340 produces by TI was used to generate the PMW (pulse width modulation) cycle, which is used to control the switch on the boost converter.

The IC also regulates the output voltage with current mode PWM control, and has an internal oscillator. Its operations as a boost converter follow as described earlier in Figure 4.11.

This work employed the use of this IC because of the minimum number of external components required to implement the design.

**Table 4.5 Boost converter (TPS55340) parameters**

| | | Value | Unit |
|---|---|---|---|
| $V_{IN}$ | DC input voltage | 3 – 5.2 | V |
| $V_{OUT}$ | DC output voltage | 18 | V |
| $I_{OUT}$ | Max Output current | 2 | A |
| $V_{OV}$ | Over Voltage –Sets maximum output voltage | 5.20 | V |
| $V_{UV}$ | Under voltage setting for shorting $V_{STORE}$ to VBAT | 3.20 | V |

#### 4.2.5.1 Component Calculations

To ensure that requirements of the boost converter are met, values for the external components must be carefully calculated.

The switching frequency of the boost converter is set by a resistor $R_{FREQ}$.

The resistor value required for a desired frequency can be calculated using:

$$R_{FREQ}(k\Omega) = 57500 \times f_{sw}(kHz)^{-1.03} \tag{4.8}$$

For the given resistor value, the corresponding frequency can be calculated by

$$f_{sw}(kHz) = 41600 \times RFREQ(k\Omega)^{-0.97} \tag{4.9}$$

$f_{sw}$ for this boost converter was chosen to 600 $kHz$. The calculated value for $R_{FREQ}$ is 78.4 kΩ and the nearest standard value resistor of 78.7 kΩ is selected.

The duty cycle at which the converter operates is given by:

$$D = \frac{V_{OUT} + V_D - V_{IN}}{V_{OUT} + V_D} \tag{4.10}$$

From calculations the maximum duty cycle was 0.85 and the minimum was 0.75.

VD is the voltage drop across the Schottky rectifier and is assumed to be 0.5.

At the minimum input of 3V, the duty cycle will be 80%. At the maximum input of 5.2V, the duty cycle is 51%.

To select an inductor, inductor value as well as DC resistance and saturation current needs to be taken into consideration. In a boost converter, maximum inductor current ripple occurs at 50% duty cycle. The maximum input current can be estimated with

$$I_{IN}DC = \frac{V_{OUT} + I_{OUT}}{\eta_{EST} + V_{IN}\min} \tag{4.11}$$

the calculated value of $I_{IN}DC$ is 4.52A.

This value is relative to $K_{IND}$ which is the coefficient that represents the amount of inductor ripple current, for this design, KIND = 0.3 and a conservative efficiency estimate of 85% with the minimum input voltage and maximum output current.

The minimum inductance is given by

$$L_o\min \geq \frac{V_{IN} + I_{OUT}}{V_{IN}DC \times K_{IND}} \times \frac{D}{f_{sw}} \tag{2.12}$$

using $V_{IN}$ $with\ D\ closest\ to$ 50% and

$$L_o\min \geq \frac{(V_{OUT} + V_D)}{V_{IN}DC \times K_{IND}} \times \frac{1}{4 \times f_{sw}} \text{ using D at 50\%} \tag{4.13}$$

The calculated value for $L_O$ is $1.659\mu H$ and a standard value of 2 $\mu H$ was chosen.

The ripple with the chosen inductance is calculated with

$$\triangle I_L = \frac{V_{IN}\min}{L_o} \times \frac{D_{\max}}{f_{sw}} \tag{4.14}$$

the value of $\Delta I_L$ was calculated to be 1.537.

The maximum output current can be evaluated with the minimum input voltage and minimum peak current limit (ILIM) of the 5.25V input as

$$I_{OUT}\,\max = \frac{V_{IN}\,\min \times \left( I_{LIM} - \frac{\triangle I_L}{2} \right) \times \eta_{EST}}{V_{OUT}} = \frac{V_{IN}\,\min \times I_{LIM} \times \left( 1 - \frac{K_{IND}}{2} \right) \times \eta_{EST}}{V_{OUT}} \quad (4.15)$$

In this design with 3V input boosted to 18V output and a $2\mu H$ inductor with an assumed Schottky forward voltage of 0.5V and estimated efficiency of 85%, the maximum output current is 630mA. With the 5.2V input and increased estimated efficiency of 90%, the maximum output current increases to 1.03A.

The output capacitance is mainly selected to meet the requirements for the output ripple ($V_{\mathrm{RIPPLE}}$) and voltage change during a load transient [37], this can be calculated using

$$C_{OUT} \geq \frac{D\,\max \times I_{OUT}}{f_{sw} \times V_{RIPPLE}} \quad (4.16)$$

To set the output voltage equation (4.17) is used, the values for $R_{SL}$ and $R_{SH}$ are selected according to the following equations

$$V_{OUT} = 1.229V \times \left( \frac{R_{SH}}{R_{SL}} + 1 \right) \quad (4.17)$$

$$R_{SH} = R_{SL} \left( \frac{V_{OUT}}{1.229V} - 1 \right) \quad (4.18)$$

For an output voltage of 18V and an optimum value for $R_{SL}$ around $10k\Omega$, the calculated value for $R_{SH}$ is $136.7k\Omega$.

The high switching frequency of the TPS55340 demands high-speed rectification for optimum efficiency. The power dissipated by the diode is given by

$$P_D = V_D \times I_{OUT} \tag{4.19}$$

With calculated $P_D = 315mA$, the recommended minimum ratings for this design are 40V, 3A diode

**Table 4.6 TPS55340 external components values**

| | |
|---|---|
| L | $2\mu H$ |
| $C_{\text{IN}}$ | $10\mu F$ |
| $C_{\text{OUT}}$ | $11.1\mu F$ |
| $R_{SH}$ | $136.7K\Omega$ |
| $R_{SL}$ | $10K\Omega$ |
| $R_{FREQ}$ | $79.1K\Omega$ |

#### 4.2.5.2 PSPICE Implementation of TPS55340

The boost converter circuit implemented in PSPICE is show as in Figure 4.14. The transient simulation model of the TPS55340 resulted in the graphs in the following figures.

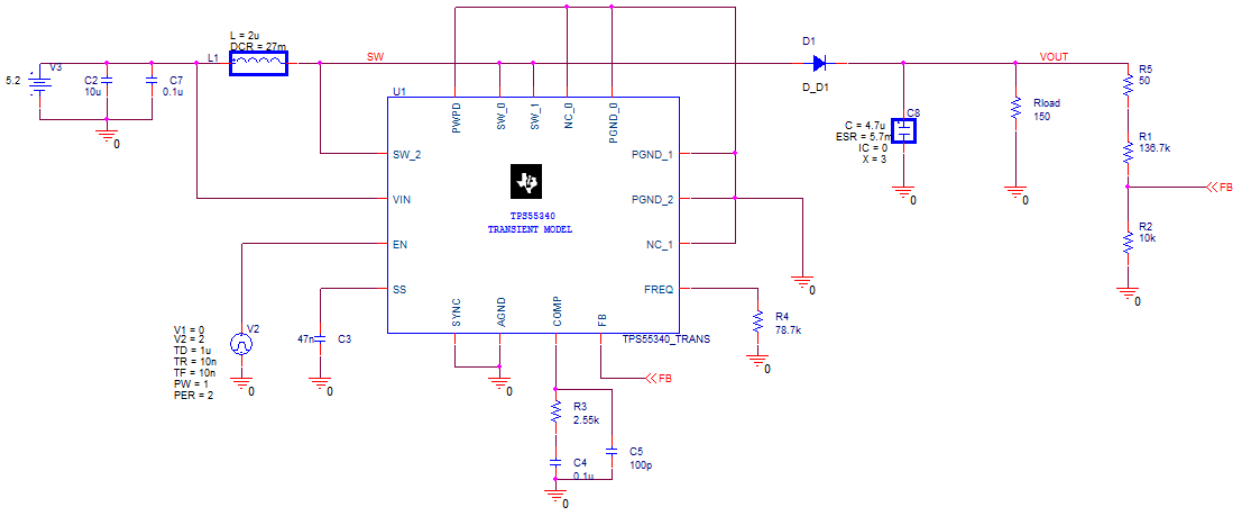


**Figure 4.14: PSPICE Simulation circuit (TPS55340).**

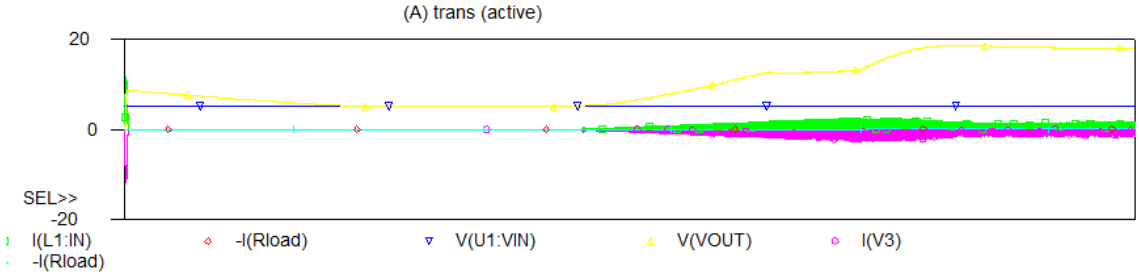


**Figure 4.15: PSPICE Simulation results (TPS55340).**

### 4.2.6 3S LiPo Battery Charger Design

3S LiPo (Lithium Polymer) is a battery pack made up of 3 individual cell each 3.7V wired together in series to produce 11.1V as in Figure 4.16.

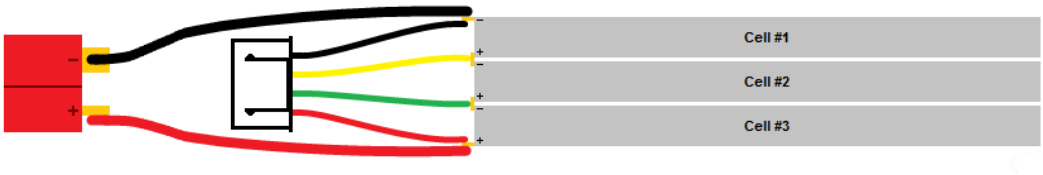


**Figure 4.16: 3S LiPo Battery wiring.**

This charger is designed to charge the 750mAH battery aboard the quadcopter; this is a 3 cell 11.1V battery which is the primary supply for the quadcopter.

#### 4.2.6.1 Proteus Implementation (3S LiPo Battery Charger)

The charger design is made up of LM317 Voltage Regulator IC used to regulate the input voltage, 5W Wire wound current regulating resistor to control input current, 120Ω resister at 1/4W MF 1% and voltage regulating resistor at 1/4W MF 1 % used to set the output voltage.

The value for the current regulating resistor $R_i$ is given by

$$R_i = \frac{1.25}{I_r} \tag{4.20}$$

Where $I_r$ is current in amps of current regulator.

For this design a 750mAH flight pack is used, the calculated value for $R_i$ is 1.67Ω, thus the value for the voltage regulating resistor $R_v$ is given by

$$R_v = (96 \times V_{OUT}) - 120 \tag{4.21}$$

For the 3 Cell pack being charged to 12.6 volts, the calculated $R_v$ value is 1090Ω.

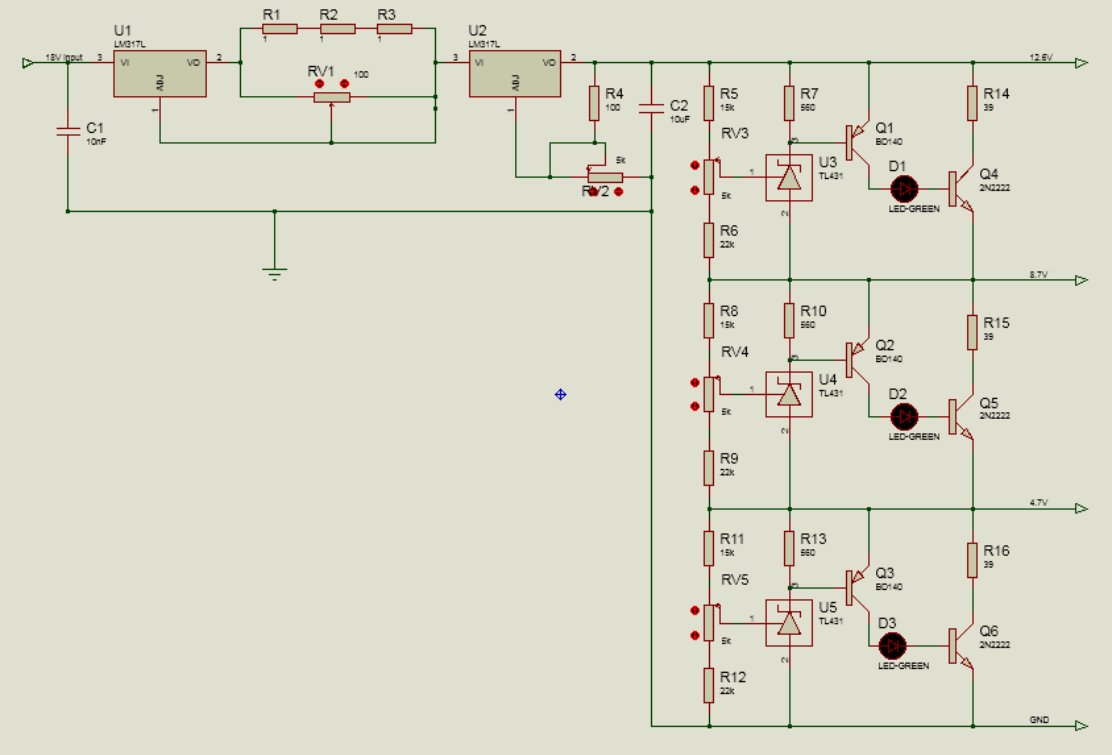


**Figure 4.17: 3S LiPo charger with balancer circuit .**

### 4.2.7 Power Consumption and Energy Storage

As motioned earlier aside the four rotor the quadcopter also carry other electronic payload which contribute to its power consumption.

The main power supply for the quadcopter is a LiPo battery, in this research a 3s 20C 750mA LiPo battery is used for testing. With a capacity of 750mAh the battery can holdup the operation of the quadcopter for an hour providing a continuous current of 0.75A. The discharge rate of the battery which is determined by the C rating is calculated as 15A continuously. To charge the battery a charge rate of 1C is assumed

since the manufacture did not provide one. At 1C the battery can be charged with a current of 0.7A for an hour.

From the experiment each rotor require 0.4A, making a total of 1.6A for 4 rotors. A total of 0.26A is also required for both the microcontroller and the Bluetooth shield.

In all a total of 1.86A is drawn from the battery during operation of the quadcopter.

With a 750mAh battery the maximum flight duration of the quadcopter can be estimated.

With constant current draw of about 2A from a 750mAh LiPo, the flight duration is calculated as $\left(750mAh\ /1000\right)\ /\ 2A\ =\ 0.375\,x\ 60\ =\ 22.5$ minutes flying time.

### 4.3 Testing and Results

Testing was done for the individual subsystems after which, the whole integrated system was tested. This section discusses the various testing process.

To verify the generator results obtained from the model, an Arduino code was written to drive a motor coupled with the BLDC generator, a load range of 10Ω to 1kΩ was applied the result is presented in Table 4.7.

**Table 4.7 Test result for BLDC generator**

| | Meter | 10Ω | 150Ω | 500Ω | 1kΩ |
|---|---|---|---|---|---|
| RPM | 5400 | 5400 | 5400 | 5400 | 5400 |
| Output Voltage | 3.2V | 3.2V | 3.2V | 3.2V | 3.2V |
| Output Current | 0.56A | 0.24A | 0.03A | 7.1mA | 3.5mA |
| Power | 1.79W | 0.768mW | 0.096W | 22.7mW | 11.2mW |

Testing of the 5.2V boost converter was done using a power supply, which represents the output of the rectification circuit. During the test the voltage supply was varied between 0.2 and 4 volts and a digital multimeter was used to measure the output voltage of the boost converter in each case, the results is presented in Table 4.8.

A similar testing process above was used to test 18V boost converter, the input voltage range was from 1.5V to 5V the results is presented in Table 4.9.

The 3s LiPo charger with balancer was also designed and tested separately. The balancing circuit is implemented to make sure each of the three cells is adequately charged. An input voltage of 18V to 20V was applied at its terminal and in all the cases the output voltage was 12.6. This result is presented in Table 4.10

**Table 4.8 Test results for 5.2 boost converter**

| Input voltage (V) | Output voltage (V) |
|---|---|
| 0.5 | 5.2 |
| 1.0 | 5.2 |
| 1.5 | 5.2 |
| 2.0 | 5.2 |
| 2.5 | 5.2 |
| 3 | 5.2 |

**Table 4.9 Test results for 18V boost converter**

| Input voltage | Output voltage |
|---|---|
| 1.5V | 7.2V |
| 2V | 15.4V |
| 3V | 20V |
| 4V | 20V |
| 5V | 20V |

**Table 4.10 Test results for 3s LiPo charger**

| Input voltage | 18V - 20V |
|---|---|
| Output | 12.6V |
| | Output voltage |
| Balancer1 | 12.6V |
| Balancer2 | 8.4V |
| Balancer2 | 4.5V |

Having verified the individual circuit units, the various units were put together and tested.

As in the case for testing the generator, an Arduino code was written to drive a motor coupled with the BLDC generator. The output of the generator was fed to the complete circuit, which gives an output of 18.03V at 0.6A.

## 4.4 Discussion of Results

Comparing the results obtained from the MATLAB model of the microgenerator and that obtained the physical model it is observed that the simulation values are a bit higher than that of the physical model, this can be attributed to the fact that the Simulink model is an ideal representation of the generator and factors such mechanical friction were not considered during modelling.

**Figure 4.18: Test setup 1.**

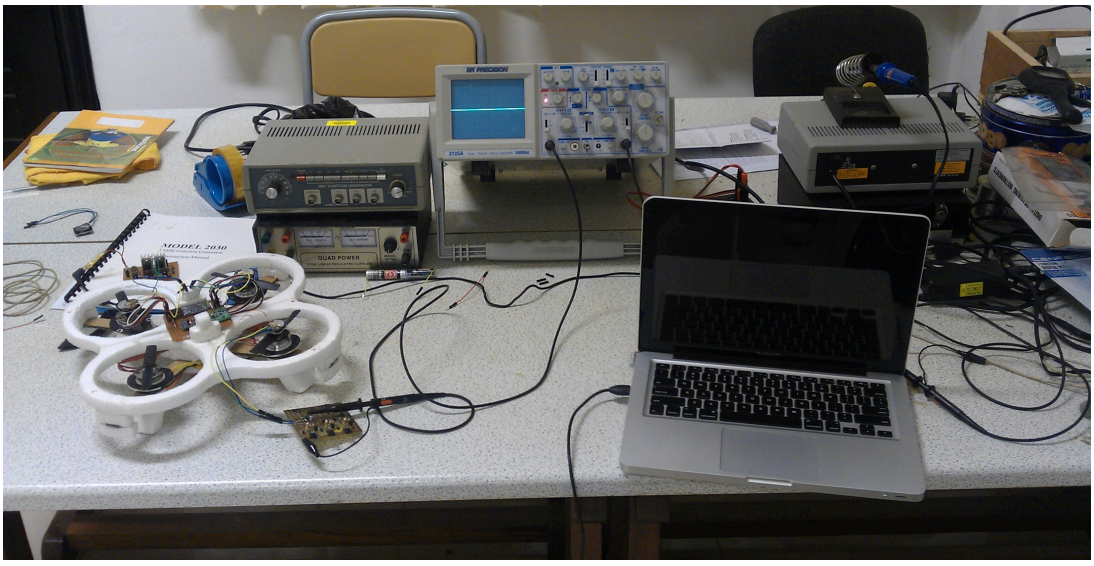

**Figure 4.19: Test setup 2**

The testing results show that with the implementation of voltage regulation, the harvester circuit performs well with slight deviation in input voltages. The 5.2 boost

converter produces regulated 5.2V with an input range from 1.5V to 3V, the 18V boost converter also produces a regulated output of 18V from a range of 3V to 5V.

The 3s LiPo battery charger with balancer circuit is able to give out an output of 12.6V output, with 8.4V, and 4.5V from the balancer section.

The harvester system produced output power levels of 4.98W at a source rotation speed of 5400RPM.

With an overall current of 2A was drawn from the battery, the results show that the Energy harvesting can add about 30% of current to the quadcopter power supply by delivering about 600mA of current from the four generators connected in parallel. This translates to about 10 minutes increase in flight endurance, thus a gain of about 50% in flight duration.

From the results obtained from testing, the power output of the generator reduces as the load resistance increases, which in effect causes reduction in efficiency. Although the configuration $Rload \gg Rsource$ achieves the maximum electrical efficiency and prevents the generator from thermal destruction, Rload cannot increase out of bounds (e.g. in case power output approaches 0W) else it will overload the generator.

# CHAPTER 5

# CONCLUSION AND RECOMMENDATION

## 5.1 Introduction

This chapter presents a summary of the work presented in this thesis, also challenges, observations and ideas for future improvements are disused.

## 5.2 Conclusions

In conclusion, all the requirement and specification has been met by the proposed design.

The work has demonstrated a rotational energy harvester powered by rotors using a BLDC generator. The mathematical model of the BLDC generator is used to analyse the waveforms of the output of the generator, results from the physical model of the generator verify the results of the mathematical model.

The BLDC generator was able to harvest continues rotation from the rotor of the quadcopter to electrical energy. At a revolution of 5400RPM, the generator produces 3.2V.

After simulating the harvester circuit the physical model was built on a PCB board.

The harvester interface circuit was able to take an input of 1.5V to 3.2V from the rectifier circuit and produce a regulated output of 18V.

About 30% of the current required to keep the quadcopter in operation is achieved form the rotational harvester, resulting in 10 minutes improvement in flight duration.

This result is achieved without any form of optimization either in the circuit implementation or in the rotational harvester.

In the end the two research questions “Can rotational energy be scavenged from the quadcopter” and “Can the energy harvested be used to power the quadcopter to increase its flight duration” has been answered.

## 5.3 Challenges and observations

One of the major challenges faced during this research was with the implementation of the system design.

Components used in the design were not sold on the local market, some of the components include:

- SMD electronic components
- 3s LiPo battery
- Arduino Microcontroller
- Copper clad PCB board
- Propellers
- High-speed BLDC motor.

- Bluetooth module

As such these components were ordered from overseas which attract very expensive shipping rate. Some were also not easy to come by, example being the microgenerator which was obtained from a crashed laptop hard disk drive.

Also coupling the generator to the rotors of the quadcopter was difficult, the process require that the axis or rotation for both the generator and the motor are perfectly align. That can be done on a lab bench fitted with a clamp.

## 5.4 Recommendations

Further work needs to be done to establish the following improvements on a rotational energy harvesting system:

- Implementing an optimization algorithm to control and match current and voltage waveforms in the generators output in order to increase power density.
- Using a gearbox to increase or decrease the RPM of the generator.

  A gearbox is needed to step up RPM in the case where the prime mover RPM is relatively low as compared to that of the generator, also a gearbox is needed in a case where the prime mover has excessive RMP that might contribute to the heating of the generator.

- A proper alignment of the generators axes of rotation to that of prime mover during the coupling process could reduce the vibrations that is introduce in to the system as a result of this process.

## REFERENCES

[1] H. Lee, "Advanced Control for Power Density Maximization of The Brushless Dc Generator," Texas A&M University, 2003.

[2] S. Beeby and W. Neil, "*Energy Harvesting for Autonomous Systems*. 685 Canton Street Norwood", MA 02062: Artech House Series, p. 304, 2010.

[3] A. S. Henry, P. G, and J. Inman D., "Estimation Of Electric Charge Out Put For Piezo Electric Energy Harvesting," *Strain*, vol. 40, no. 2, pp. 49–58, 2004.

[4] S. S. Rao and M. Sunar, "Analysis Of Distributed Thermopiezoelectric Sensors And Actuators In Advanced Intelligent Sensors," *AIAA J.*, vol. 31, no. 7, pp. 1280–1286, 1993.

[5] S. R. Anton and H. A. Sodano, "A Review of Power Harvesting Using Piezoelectric Materials," *Smart Mater. Struct.*, vol. 16, no. 3, pp. R1–R21, 2007.

[6] H. W. Kim, A. Batra, and S. Priya, "Energy Harvesting Using A Piezoelectric 'Cymbal' Transducer In Dynamic Environment," *Jpn. J. Appl. Phys.*, vol. 43, no. 9A, pp. 6178–6183,, 2003.

[7] S. Roundy and P. K. Wright, "A Piezoelectric Vibration Based Generator for Wireless Electronics," *Smart Mater. Struct.*, vol. 13, pp. 1131–1142, 2004.

[8] N. S. Shenck and J. A. Paradiso, "Energy Scavenging With Shoe-Mounted Piezoelectrics," *IEEE Micro*, vol. 21, no. 3, pp. 30–42, 2001.

[9] K. Park, M. Lee, Y. Liu, S. Moon, G. Hwang, G. Zhu, J. E. Kim, S. O. Kim, D. K. Kim, Z. L. Wang, and K. J. Lee, "Flexible Nanocomposite Generator Made of BaTiO 3 Nanoparticles and Graphitic Carbons," vol. 24, no. 22, 2012.

[10] A. S. Holmes, G. Hong, and K. R. Pullen, "Axial-Flux Permanent Magnet Machines For Micropower Generation," *J. Microelectromechanics Syst.*, vol. 15, no. 1, pp. 54–62, 2005.

[11] W. S. N. Trimmer, "Microrobots and micromechanical systems," *Sensors and Actuators*, vol. 19, no. 3, pp. 267–287, 1989.

[12] H. Raisigel, O.´e Cugat, and J.´roˆme Delamare, “Permanent Magnet Planar Micro-Generator,” *Sensors Actuators A Phys.*, vol. 130–131, pp. 438–444, 2006.

[13] W. S. N. Trimmer and K. J. Gabriel, “Design Considerations for A Practical Electrostatic Micro-Motor,” *Des. considerations a Pract. Electrost. micro-motor*, vol. 11, no. 2, pp. 189–206, 1987.

[14] T. T. Toh, “A Gravitational Torque Energy Harvesting System for Rotational Motion,” Imperial College London, 2011.

[15] J. Long, “Complex Conjugate Match False Fetish,” 2012. [Online]. Available: http://www.analog-rf.com/match.shtml. [Accessed: 17-Jun-2014].

[16] L. Wang, T. Kazmierski, B. Al-Hashimi, and et al, “An Integrated Approach to Energy Harvester Modeling and Performance Optimization,” *IEEE Behav. Model. Simul. Conf. (BMAS 2007)*, vol. San Jos, no. California, pp. 121–125, 2007.

[17] H. Yan, J. G. M. Montero, and A. Akhnoukh, “An Integration Scheme for RF Power Harvesting,” *STW Annu. Work. Semicond. Adv. Futur. Electron. Sensors*, pp. 64–66, 2005.

[18] P. D. Mitcheson, T. C. Green, and E. M. Yeatman, “Power processing circuits for electromagnetic, electrostatic and piezoelectric energy scavengers,” *Microsyst. Technol.*, vol. 13, pp. 1629–1635, 2007.

[19] L. Garbuio, M. Lallart, and D. Guyomar, “Mechanical Energy Harvester with Ultralow Threshold Rectification Based on SSHI Nonlinear Technique,” *IEEE Trans. Ind. Electron.*, vol. 56, no. 4, pp. 1048–1056, 2009.

[20] E. H. Technologies, “MEMS Electrostatic Micropower Generator for Low Frequency Operation,” *Sensors Actuators A Phys.*, vol. 115, no. 2–3, p. Sensors and Actuators A: Physical, 2004.

[21] E. Lefeuvre, D. Audigier, C. Richard, and D. Guyomar, “Buck-Boost Converter For Sensorless Power Optimization Of Piezoelectric Energy Harvester,” *IEEE Trans. Power Electron.*, vol. 22, no. 5, pp. 2018–2025, 2007.

[22] E. M. Yeatman, "Energy Harvesting from Motion Using Rotating and Gyroscopic Proof Masses," *Proc. Inst. Mech. Eng. Part C J. Mech. Eng. Sci.*, vol. 22, no. 1, pp. 27–36,, 2008.

[23] P. Mitcheson, T. C. Green, E. M.Yeatman, and H. A. S., "Architectures For Vibration Driven Micropower Generators," *J. Microelectromechanic Syst.*, vol. 13, no. 3, pp. 429–440, 2004.

[24] Perpetuum, "PMG37 Vibration Energy Harvester." 2010.

[25] U. Bartsch, J. Gaspar, and O. Paul, "Low-Frequency Two-Dimensional Resonators for Vibrational Micro Energy Harvesting," *J. Micromechanics Microengineering*, vol. 20, no. 3, p. 035016, 2010.

[26] P. D. Mitcheson, P. Miao, B. H. Stark, and et al, "MEMS Electrostatic Micropower Generator for Low Frequency Operation," *Sensors Actuators A Phys.*, vol. 15, no. 2–3, pp. 523–529, 2004.

[27] A. Ferrero and G. Superti-Furga, "A New Approach to the Definition of Power Components in Three-phase Systems under Nonsinusoidal Conditions," *IEEE Trans. Instrum. Meas.*, vol. 40, no. 3, pp. 568–577, 1991.

[28] O. Liang, "Build A Quadcopter From Scratch - Hardware Overview," 2013. [Online]. Available: http://blog.oscarliang.net/build-a-quadcopter-beginners-tutorial-1/. [Accessed: 21-Jun-2014].

[29] "File: Rollpitchyawplain.png - Wikipedia." [Online]. Available: http://en.wikipedia.org/wiki/File:Rollpitchyawplain.png. [Accessed: 21-Jun-2014].

[30] T. J. Coyle, "The World's First Solar Powered Quadcopter," 2013. [Online]. Available: http://diydrones.com/profiles/blogs/the-world-s-first-solar-powered-quadcopter. [Accessed: 27-May-2014].

[31] M. Grady, "Solar Drone Sets Endurance Record," 2010.

[32] S. R. Anton, "Novel Piezoelectric Energy Harvesting Devices for Unmanned Aerial Vehicles," pp. 1–10, 2009.

[33] S. R. Anton and D. J. Leo, "Multifunctional Piezoelectric Energy Harvesting Concepts by Multifunctional Piezoelectric Energy Harvesting Concepts," 2011.

[34] A. Tashakori, M. Iaeng, M. Ektesabi, and N. Hosseinzadeh, “Modeling of BLDC Motor with Ideal Back- EMF for Automotive Applications,” vol. II, pp. 4–8, 2011.

[35] S. Baldursson, “BLDC Motor Modelling and Control – A Matlab / Simulink Implementation,” Institutionen för Energi och Miljö, 2005.

[36] TI, “Ultra Low Power Boost Converter with Battery Management for Energy Harvester Applications (BQ25504 Data sheet),” 2012.

[37] TI, “Integrated 5-A 40-V Wide Input Range Boost/SEPIC/Flyback DC-DC Regulator,” 2013.

[38] “Controlling Brushless Motor: Arduino,” 2012. [Online]. Available: http://www.element14.com/community/thread/19879/l/controlling-brushless-motor. [Accessed: 29-Jul-2014].

# APPENDIX A

## Software Interfaces: Eagle PCB Design

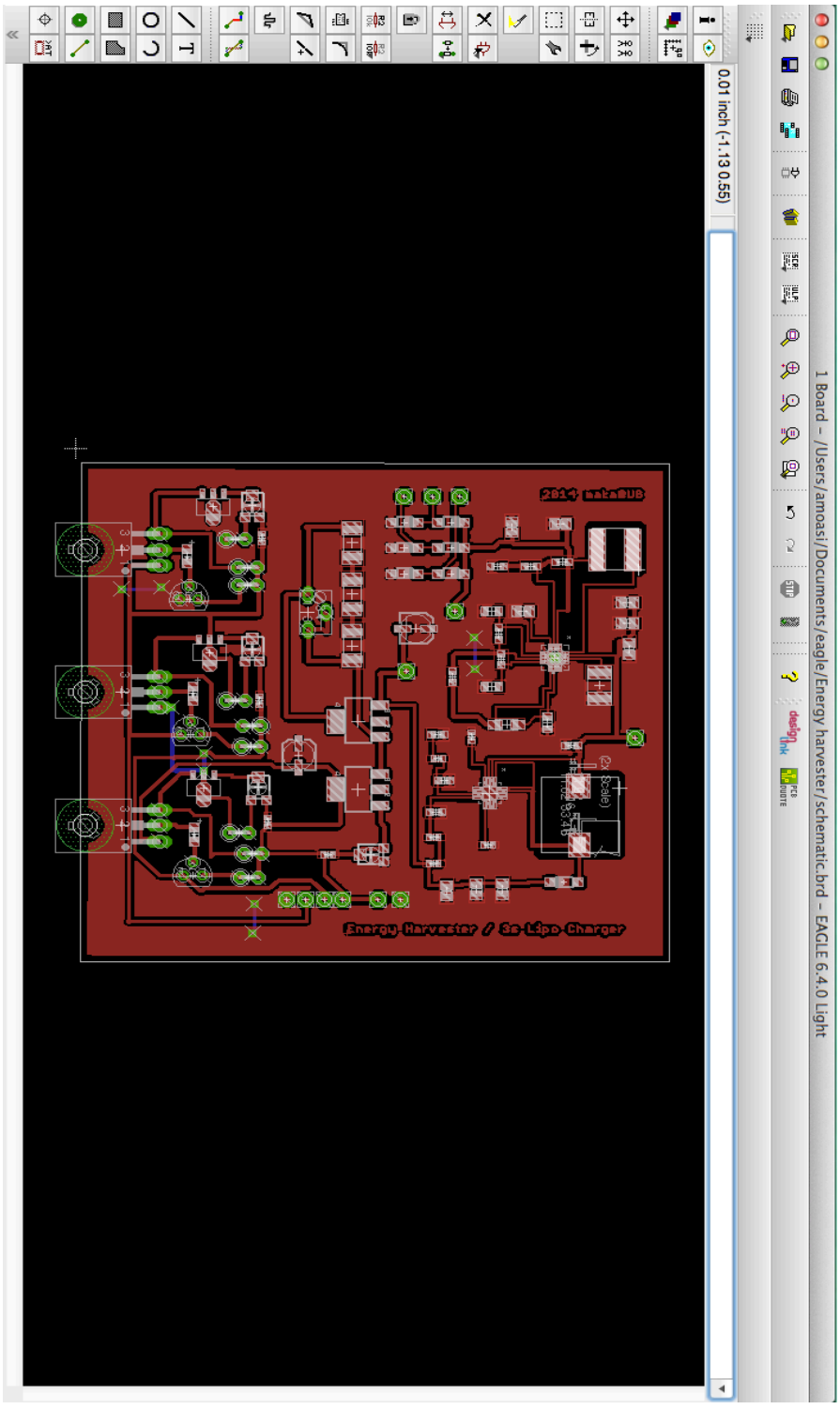

**Software Interfaces: Eagle Circuit Design**

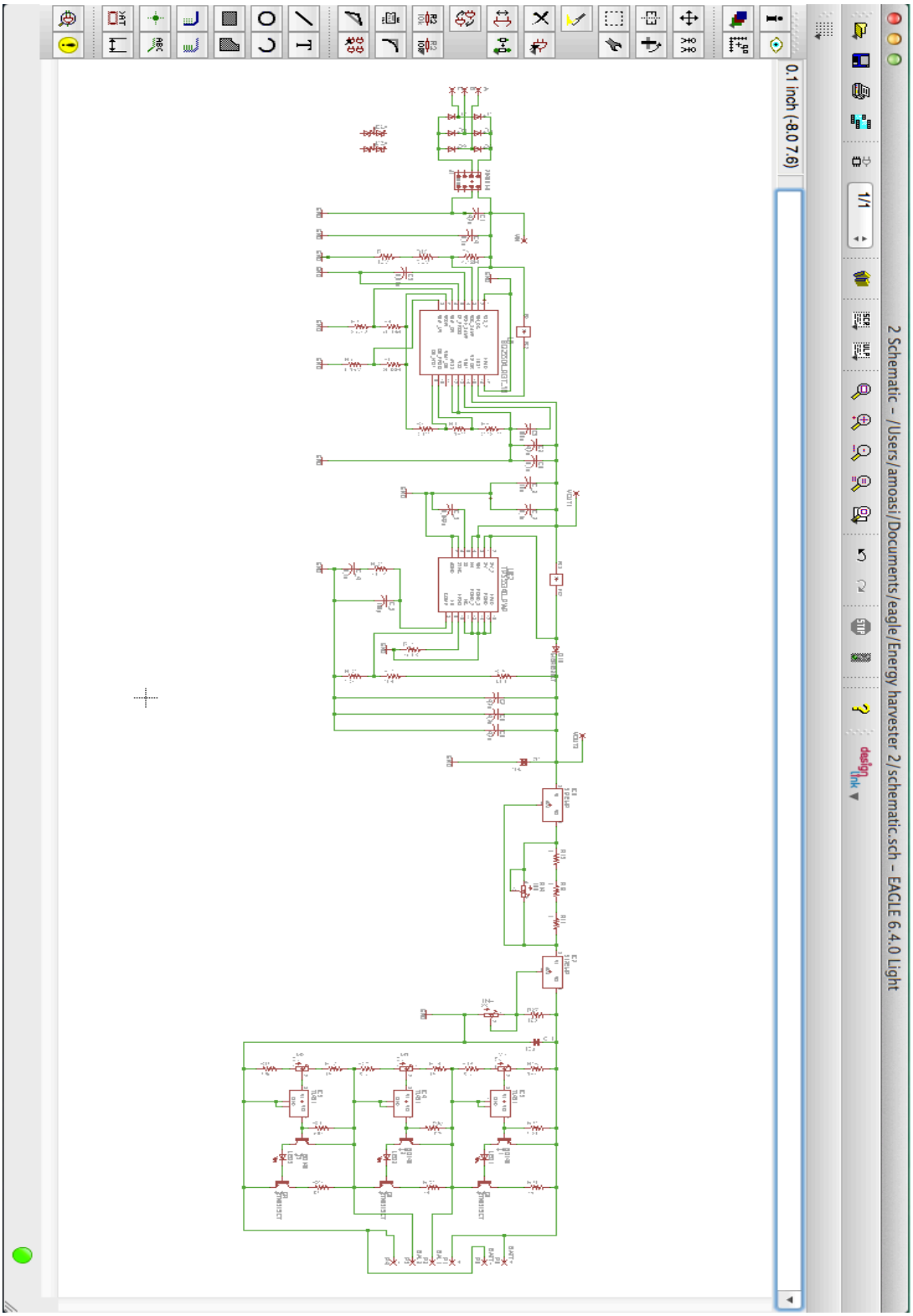

# APPENDIX B

## List of Development Tools

| **Software Tools** |
|---|
| Matlab R2012a® |
| Arduino 1.0.5 |
| Eclipse JUNO |
| Cadsoft Eagle 6.4.0 |
| Cadence PSPICE 16.3 |
| |
| |
| **Hardware Tools** |
| Arduino Pro Mini 328 - 5V/16MHz + usb programmer |
| Nintendo Motion Plus Sensor Adapter |
| TURNIGY Plush 10amp 9gram Speed Controller |
| Rhino 750mAh LiPo Pack |
| GWS EP Propeller (RD-1047 254x119mm) (6pcs/set) |
| 5.4x4.3 Propeller (Standard and counter clockwise) |
| Battery strap |
| HC-05 Embedded Bluetooth Serial Comm. Module |
| Programming card |
| Styrofoam frame |
| |
| |
| **PCB Materials** |
| Photopaper |
| Isopropanol |
| Ferric Chlorid |
| Acetone |
| Liquid Tinner |
| Copper clad board 12x12 |
| Beaker |
| Gloves |
| |
| |
| **Tools** |
| Up to10X magnifying headset loupe magnifier |
| SMD reworkstation |
| thin wire |
| Bostik Blu Tack Removeable Adhesive 75 Gram |
| 0.5" diameter solder |
| fine point tweezer |
| Multi-meter |

| |
|---|
| Screw driver set |
| Power Supply |
| |
| |
| **SMD Electronic Components** |
| BQ25504 Ultra Low Power Boost Converter |
| TPS55340 Boost Converter |
| Inductors |
| Capacitors |
| Transistors |
| Trimmers |

# APPENDIX C

Part of Arduino Code for Testing

(Modified: [38])

```
#include "Servo.h"

#define MOTOR_PIN                13

#define MOTOR_MAX_SPEED          180

#define MOTOR_START_SPEED        80


int motor_current_speed = 0;

int motor_increment = 1;

int max_reached = 0;


Servo motor;


void motorSetSpeed(int speed)

{

        if (speed &gt; MOTOR_MAX_SPEED)

         speed = MOTOR_MAX_SPEED;

        else if (speed &lt; MOTOR_START_SPEED)

         speed = MOTOR_START_SPEED;


        motor.write(speed);
```

```
        motor_current_speed = speed;


        Serial.print("current motor speed = ");

        Serial.println(motor_current_speed);

}


void motorSpeedUp()

{

        int increment = (motor_current_speed &lt; 100) ? motor_increment + 3:
        motor_increment

        motorSetSpeed(motor_current_speed + increment);

}


void motorSlowDown()

{

        motorSetSpeed(motor_current_speed - increment);

}


void motorStop()

{

        motor.write(0);

}
```

```
void motorStartAt(int start_speed)
{
        int i;
        for (i=0; i &lt; start_speed; i+=5) {
         motorSetSpeed(i);
         Serial.println(i);
         delay(100);
        }
}

void setup()
{
        // Setup init
        Serial.begin(9600);

        // Motor
        delay(1000);
        motor.attach(MOTOR_PIN);
        motorStartAt(motor_start_speed);
        delay(1500);
}
```

```
void loop()

{



    if (!max_reached) {

       motorSpeedUp();

    } else {

       motorSlowDown();

    }

    if (motor_current_speed &lt; MOTOR_START_SPEED) {

       max_reached = 0;

    } else if (motor_current_speed &gt; MOTOR_MAX_SPEED) {

       max_reached = 1;

    }

    delay(500);

}
```